Regional scale tree-ring reconstructions of hydroclimate dynamics and Pacific salmon abundance in west central British Columbia

by

Colette Christiane Angela Starheim
B.A., University of British Columbia, 2008

A Thesis Submitted in Partial Fulfillment of the
Requirements for the Degree of

MASTER OF SCIENCE

in the Department of Geography

Supervisory Committee

Regional scale tree-ring reconstructions of
hydroclimate dynamics and Pacific salmon abundance
in west central British Columbia

by

Colette Christiane Angela Starheim
B.A., University of British Columbia, 2008

Supervisory Committee

Dr. Dan J. Smith, (Department of Geography)
Co-supervisor

Dr. Terry D. Prowse, (Department of Geography)
Co-supervisor

Supervisory Committee

Dr. Dan J. Smith, (Department of Geography)
Co-supervisor

Dr. Terry D. Prowse, (Department of Geography)
Co-supervisor

Abstract

Long-duration records are necessary to understand and assess the long-term dynamics of natural systems. The purpose of this research was to use dendrochronologic modelling to construct proxy histories of hydroclimatic conditions and Pacific salmon abundance in west central British Columbia. A multi-species regional network of tree ring-width and ring-density measurements was established from new and archived tree-ring chronologies. These chronologies were then used in multivariate linear regression models to construct proxy records of nival river discharge, summer temperature, end-of-winter snow-water equivalent (SWE), the winter Pacific North America pattern (PNA) and Pacific salmon abundance.

All proxy hydroclimate records provide information back to 1660 AD. Reconstructions of July-August mean runoff for the Skeena and Atnarko rivers describe below average conditions during the early- to mid-1700s and parts of the early-, mid- and late-1900s. Models describe intervals of above average river discharge during the late-1600s, the early-1700s and 1800s, and parts of the early- and mid-1900s. Fluctuations in proxy reconstructions of July-August mean temperature for Wistaria and Tatlayoko Lake, May 1 SWE at Mount Cronin and Tatlayoko Lake and October-February PNA occurred in near synchrony with the shifts described in runoff records. Episodes of above average runoff were typically associated with periods of enhanced end-of-winter SWE, below average summer temperature and positive winter PNA.

A history of Pacific salmon abundance was reconstructed for four species of salmon (chinook, sockeye, chum and pink) that migrate to coastal watersheds of

west central British Columbia. Proxy records vary in length and extend from 1400 AD, 1536 AD and 1638 AD to present. Salmon abundance reconstructions varied throughout the past six centuries and described significant collapse in population levels during the early-1400s, the late-1500s, the mid-1600s, the early-1700s, the early-1800s and parts of the 1900s.

Wavelet analyses of reconstructed hydroclimate and salmon population records revealed low- and high-frequency cycles in the data. Correlation analyses related reconstructions to atmospheric teleconnection indices describing variability in North Pacific sea surface temperatures and the Aleutian Low pressure centre. To a lesser degree, relationships were also established between reconstructions and the El Niño-Southern Oscillation. Results thus confirm the long-term influence of large-scale ocean and atmospheric circulation patterns on hydroclimate and Pacific salmon abundance in west central British Columbia.

The reconstructions introduced in this thesis provide insights about the long-term dynamics of the west central British Columbia environment. Several reconstructions presented in this thesis provide novel contributions to dendrohydroclimatic and paleoecologic research in Pacific North America. Proxy runoff records for the Skeena and Atnarko rivers are the first to be constructed for nival-regime basins in British Columbia. The models of Skeena River runoff and Mount Cronin SWE are additionally the first reconstructions of runoff and snowpack in Pacific North America based on a ring-density chronology, demonstrating the significant contribution that wood density measurements can make to dendrohydroclimate research. The models of Pacific salmon stocks are the first to utilize climate-sensitive tree-ring records to construct a history of regional salmon abundance and thus represent a significant advancement to paleoecological modelling.

Table of Contents

Supervisory Committee ii

Abstract iii

Table of Contents v

List of Tables vii

List of Figures viii

Acknowledgements xi

Dedication xiii

1. Introduction 1
1.1. Introduction 1
1.2. Research Objectives 3
1.3. Thesis Outline 3

2. Dendrohydroclimate reconstructions of melt-season runoff for two nival-regime rivers in west central British Columbia 5
2.1. Introduction 5
2.2. Study Area 7
2.3. Methods and Data 11
2.3.1. Hydroclimate and Atmospheric Teleconnection Index Data 12
2.3.2. Tree-Ring Data 12
2.3.3. Dendrohydroclimate Correlations and Reconstructions 15
2.4. Results 17
2.4.1. Tree-Ring Chronologies 17
2.4.2. Hydroclimate Correlations within the Instrumental Record 19
2.4.3. Dendrohydroclimate Correlations 21
2.4.4. Hydroclimate Reconstructions 23
2.5. Discussion 27
2.5.1. Hydroclimate Correlations within the Instrumental Record 27
2.5.2. Dendrohydroclimate Correlations 28
2.5.3. Hydroclimate Reconstructions 30
2.5.4. Connections to Large-Scale Ocean and Atmospheric Forcings 31
2.5.5. Comparisons to Other Paleohydroclimate Records 34
2.6. Conclusion 35

3. Regional scale reconstructions of Pacific salmon abundance for west central British Columbia using climate-sensitive tree-ring records 38
3.1. Introduction 38
3.2. Research Background 40
3.3. Study Area 41
3.4. Data and Methods 44
3.4.1. Tree-Rings and Large-Scale Climate 44
3.4.2. Pacific Salmon and ATI Data 47
3.4.3. Relationships Between Tree-Rings, ATIs and Pacific Salmon 48
3.4.4. Reconstructions of Pacific Salmon Abundance 50
3.5. Results 51
3.5.1. Tree-Ring Chronologies 51
3.5.2. Relationships Between Tree-Rings, ATIs and Pacific Salmon 52
3.5.3. Reconstructions of Pacific Salmon Abundance 55
3.6. Discussion 60
3.6.1. Reconstructions of Pacific Salmon Abundance 60
3.6.2. Comparisons of Other Proxy Records of Salmon Abundance 62
3.6.3. Climate Connections 63
3.7. Conclusion 63

4. Summary and Conclusion 65
4.1. Summary of Findings 65
4.1.1. Hydroclimate Reconstructions 65
4.1.2. Pacific Salmon Reconstructions 67
4.2. Runoff, Climate and Pacific Salmon Connections 68
4.3. Research Limitations and Opportunities 69
4.3.1. Improving Models for Salmon Abundance 69
4.3.2. Comparing Multiple Tree-Ring Proxy Records 70
4.3.3. Spatial Coverage of a Regional Tree-Ring Network 71
4.3.4. Building a Multi-Species Ring-Density Network 71
4.3.5. Century-Scale Growth Patterns 73
4.4. Conclusion 73

References Cited 74

Appendices 83
A Climate Reconstruction Calibration Diagrams 83
B Climate Reconstruction Wavelet Power Spectrum Diagrams 84
C Exploratory Model of Salmon Abundance Using Catch Records 85
D Exploratory Correlation Analyses with Ring-Density Chronologies 87
E Century-Scale Growth of Yellow Cedar and Whitebark Pine Trees 88

List of Tables

2.1 Hydroclimate station locations 10

2.2 Tree-ring chronology sampling locations 17

2.3 Summary statistics for individual and regional tree-ring chronologies 19

2.4 Summary statistics for hydroclimate reconstructions 25

2.5 Correlations between reconstructed records and ATIs 32

3.1 Salmon escapement regions 48

3.2 Tree-ring chronology sampling location 52

3.3 Summary statistics for master tree-ring chronologies 52

3.4 Statistically significant correlations between master tree-ring chronologies and ATIs 53

3.5 Correlations between salmon escapement records and ATIs 54

3.6 Summary statistics for salmon reconstructions 56

4.1 Correlations between Skeena River discharge and salmon escapement 69

4.2 Chronology statistics for yellow cedar and whitebark pine maximum ring-density chronologies 72

D.1 Comparative correlation strength of ring-width and maximum ring-density chronologies to Tatlayoko Lake temperature 87

List of Figures

2.1 Map of west central British Columbia study region 8

2.2 Standardized and residual master tree-ring indices. Solid black lines represent standardized data, dashed gray lines represent residual data. Blue line indicates sample depth. 20

2.3 Significant Pearson's correlation coefficients between master tree-ring chronologies and monthly hydroclimate records ($p \leq 0.05$). All months in lower case letters represent months from the year preceding growth. Where both standardized and residual chronologies significantly correlate to records only the strongest relationship is reported. Correlations marked by * are calculated using residual chronologies..... 22

2.4 Comparison between reconstructed (black line) and instrumental (gray line) records of July-August mean runoff for the Skeena and Atnarko rivers during the calibration period..... 24

2.5 Reconstructions of west central British Columbia hydroclimate anomalies from 1660 AD to present. Gray lines are the actual reconstructions while the black lines represent a 10-year running mean of the data. Shaded gray areas illustrate intervals typically exhibiting above average July-August runoff..... 26

2.6 Wavelet power spectrum for the Skeena and Atnarko runoff reconstructions. The wavelet power spectrum uses a Gaussian-2 function. Cross-hatched regions of the wavelet diagrams represent the cone of influence where zero-padding of the data was used to reduce variance. Black contours indicate significant modes of variance with a 5% significance level using an autoregressive lag-1 red-noise background spectrum (Torrence and Compo, 1998) 33

3.1 Map of the west central British Columbia coastline. The three areas outlined in black represent the approximate terrestrial boundaries for the three regional populations of Pacific salmon examined in this study, the Bulkley River (BR), North Coastal Islands (NCI), and the Dean and Burke Channels (DBC)..... 42

3.2 Significant correlations for the six regional populations of Pacific salmon reconstructed and master tree-ring chronologies. Where both standardized and residual master chronologies significantly correlate to Pacific salmon records only the strongest relationship is reported. The correlation denoted by a * represents a result where the strongest correlation was calculated using the residual master chronology 55

3.3 Reconstructions of salmon abundance anomalies. Gray lines are the actual reconstructions. Black lines represent a 10-year running mean of the data. Shaded gray areas illustrate intervals of synchroneity among salmon records.....57

3.4 Wavelet power spectrums for the six salmon abundance reconstructions. The wavelet power spectrum uses a Gaussian-2 function. Cross-hatched regions of the wavelet diagrams represent the cone of influence where zero-padding of the data was used to reduce variance. Black contours indicate significant modes of variance with a 5% significance level using an autoregressive lag-1 red-noise background spectrum (Torrence and Compo, 1998) 59

3.5 Seven-year running mean trend lines of the six escapement records modelled using climate-sensitive tree-ring measurements..... 61

A.1 Comparison between reconstructed (black line) and instrumental (gray line) records of summer temperature, SWE and PNA during the calibration period..... 83

B.1 Wavelet power spectrum for temperature, SWE and PNA reconstructions. The wavelet power spectrum uses a Gaussian-2 function. Cross-hatched regions of the wavelet diagrams represent the cone of influence where zero-padding of the data was used to reduce variance. Black contours indicate significant modes of variance with a 5% significance level using an autoregressive lag-1 red-noise background spectrum (Torrence and Compo, 1998) 84

C.1 Comparison between reconstructed (black) and instrumental (gray) records of Pacific salmon abundance for chinook, pink and sockeye returning to the Skeena River (including both escapement and catch records) during the calibration period 86

C.2 Reconstruction of Pacific salmon abundance (chinook, pink and sockeye) returning to the Skeena River back to 1660 AD, calibrated from salmon catch and escapement records 86

E.1 Growth anomalies of the yellow cedar (gray line) and whitebark pine (black line) ring-width chronologies 88

E.2 Wavelet power spectrum for yellow cedar and whitebark pine chronologies. The wavelet power spectrum uses a Gaussian-2 function. Cross-hatched regions of the wavelet diagrams represent the cone of influence where zero-padding of the data was used to reduce variance. Black contours indicate significant modes of variance with a 5% significance level using an autoregressive lag-1 red-noise background spectrum (Torrence and Compo, 1998) 90

E.3 Wavelet-filtered records of whitebark pine (solid gray lines) yellow cedar (solid black lines) and sunspot numbers (dashed black lines). Data have been transformed twice, the first transformation, represented with the thin lines, involved running a 70-120 year frequency wavelet-filter. The second transformation, represented with the thicker lines, involved running a 150-250 year frequency wavelet-filter. Shaded areas represent recognized intervals of sunspot minima 92

Acknowledgements

As with any of life's big adventures, this thesis would not be what it is today without the support of many people.

For their continual guidance and assistance, I give my sincere thanks to my thesis supervisors, Dan Smith and Terry Prowse. Dan, your constant support and encouragement both in the field and back at the UVTRL has been second to none. Terry, your thoughtful insights and advice throughout the research process have been invaluable. Thank you both for everything.

An enormous thank you to all of the lovely ladies of the lab, Jodi Axelson, Bethany Coulthard, Jess Craig, Jill Harvey, Kira Hoffman, Kate Johnson, Mel Page, Kyla Patterson and Kara Pitman. Your ongoing encouragement over the past several years has been astounding. I feel so lucky to have learned something from each one of you phenomenal women. A second thank you is owed to each of you ladies for your tolerant acceptance of all my bizarre idiosyncrasies, garbage bag caves and cheese and jalapeño breakfasts included.

I thank the 2010 UVTRL field team, Dan, Jill, Jess, Jodi, Kara and Mel. This research would not have been possible without the incredible teamwork and field support that you provided. Your tree-coring muscles amaze me!

For their initial and continued support I thank Fes de Scally and Ian Saunders. I truly appreciate both your friendship and the time that you have both invested in me throughout my undergrad, it has helped to guide me where I am today.

I acknowledge a great number of others who are deserving of my gratitude. For their incredible hospitality while the UVTRL stayed in the beautiful Bella Coola Valley, I thank our gracious hosts Steve and Cheryl Waugh of Suntree Guest Cottages. I thank the wonderful pilots and staff from West Coast Helicopters in Bella Coola for the *almost* turbulence-free flights to some of our more remote sampling locations. For his insight on sampling locations in the Bella Coola Valley, I thank David Flegel from the British Columbia Ministry of Forests and Range. I thank Barbara Spencer, Bruce Baxter and David Peacock from the Canadian Department of Fisheries and Oceans for providing the Pacific salmon escapement datasets used in this thesis.

Research funding from the University of Victoria, the National Sciences and Engineering Research Council of Canada and the Canadian Foundation for Climate and Atmospheric Sciences Western Canadian Cryospheric Network is gratefully acknowledged. I thank Kelly Penrose, Sonya Larocque, Ze'ev Gedalof and Qu-Bin Zhang for the use of their chronologies, thoughtfully archived in the UVTRL tree-ring database. Another huge thank you to Ole Heggen for graciously providing the beautiful maps that accompany this research. You truly are an artist.

To my family, I give my gratitude for your understanding, support and encouragement. I love you all.

Finally, I save my most heartfelt thank you for Allan. Your unending support has taken so many forms not the least of which include your unpaid research assistance, friendship, patience and love. It may have been best said by Fes… you should probably be nominated for a sainthood. Wherever life's journey takes me I am thankful you are by my side.

Dedication

For Allan.
A squirrel among chipmunks.

Chapter 1

Introduction

1.1 Introduction

Significant fluctuations in meteorologic and oceanic conditions, river discharge, and Pacific salmon stocks characterize Pacific North American records throughout the last century (Mantua *et al.*, 1997; Kiffney *et al.*, 2002; Irvine and Fukuwaka, 2011). Marked shifts in these environmental variables are shown to track low-frequency changes in sea surface temperatures (SSTs) and the strength and location of the Aleutian Low pressure centre (Mantua *et al.*, 1997; Overland *et al.*, 1999; Stahl *et al.*, 2006). Records from the 20th Century establish the presence of three low-frequency regime shifts during the mid-1920s, the late-1940s and the late-1970s (Moore and McKendry, 1996; Mantua *et al.*, 1997).

Investigations using both instrumental and proxy records describe a differential response in streamflow, climate and salmon populations to shifts in SSTs and atmospheric pressure systems between northern and southern locations (Moore and McKendry, 1996; Mantua *et al.*, 1997; Gedalof and Smith, 2001a; D'Arrigo *et al.*, 2003). The hydroclimatic regime of west central British Columbia falls within the transitional latitudes between the two response zones

and is, in comparison to these northern and southern regions, poorly understood. Longer records are required to better understand the long-term influence of these large-scale shifts in synoptic forcings on the river discharge, climatic conditions and resident salmon population levels characterizing west central British Columbia.

Dendrochronologic modelling of hydroclimatic variables provides a valuable opportunity to extend limited records using annual differences in tree-ring growth (Fritts, 1976). Recent tree-ring research has been particularly useful in detailing past regime shifts in Pacific North American hydroclimate systems (Larocque and Smith, 2005; Coulthard, 2009; Hart *et al.*, 2010; Johnson, 2010). While this previous research has established the value of using ring-width measurements in paleohydroclimate models (e.g. Hart *et al.*, 2010), the use of ring-density measurements in this region remains largely unexplored.

Recent paleoecological studies have demonstrated the utility of reconstructing records of Pacific salmon abundance to examine long-term trends in population levels (Drake *et al.*, 2009; Gregory-Eaves *et al.*, 2009). For example, proxy records have been constructed using varying nutrient concentrations in lake sediments (Finney, 1998; Finney *et al.*, 2000) and nutrient-limited ring-width measurements from climate-insensitive riparian trees (Drake *et al.*, 2002; Drake and Naiman, 2007). Due to the nature of the predictor variables used, insights from these reconstructions are, unfortunately, limited spatially to small nursery lakes and spawning streams. At a larger regional scale, the synchrony of shifts between large-scale ocean and atmospheric circulation patterns and salmon abundance levels (Beamish and Bouillon, 1993;

Gargett, 1997; Downton and Miller, 1998) provides an additional opportunity to use climate-sensitive tree-ring measurements to reconstruct past climate-related shifts in salmon stocks.

1.2 Research Objectives

The purpose of this research was to provide insight about the long-term trends characterizing past river discharge and Pacific salmon population levels in west central British Columbia using regional records of tree-ring growth. To accomplish this, five specific objectives were defined to frame the research. These included, to: 1) build a multi-species regional network of tree-ring growth for west central British Columbia using new and archived tree-ring chronologies; 2) construct long-term, tree-ring derived records of spring freshet for nival rivers draining west central British Columbia and use these records to identify historic trends in river discharge; 3) assess the long-term influence of large-scale ocean and atmospheric forcings, air temperature and winter snow accumulation on the spring flow-regimes of these nival basins; 4) construct a history of Pacific salmon abundance for regional populations spawning along the west central British Columbia coastline using climate-sensitive tree-ring measurements; and, 5) evaluate the long-term influence of large-scale ocean and atmospheric oscillations on trends in Pacific salmon stocks.

1.3 Thesis Outline

This thesis is comprised of four chapters. The first provides an introduction to the research, outlines the purpose and objectives of the project,

and summarizes the general presentation format. The two subsequent chapters contain the main research components of the thesis and have been written in the format of scientific manuscripts for submission to relevant peer-reviewed journals. Chapter Two presents the research undertaken to develop proxy reconstructions of late melt-season flows for selected nival rivers draining west central British Columbia. It discusses long-term relationships between melt-season runoff and summer air temperatures, end-of-winter snow-water equivalent values, and atmospheric teleconnection indices. Chapter Three describes the research involved with generating long-term reconstructions of Pacific salmon abundance in three sub-regions of the west central British Columbia coastline. It describes a novel method for building proxy records of salmon abundance at a regional scale using climate-sensitive tree-ring measurements. The fourth and final chapter summarizes the key research findings, suggests connections between the two main research contributions, provides discussion on research limitations, and offers insight about future research opportunities.

Chapter 2

Dendrohydroclimate reconstructions of melt-season runoff for two nival-regime rivers in west central British Columbia

2.1 Introduction

The annual discharge regime of rivers and streams in British Columbia varies substantially from year-to-year. In coastal and interior regions a significant component of this behaviour is attributed to the varied impact of large-scale ocean and atmospheric climate oscillations (Moore, 1996; Kiffney *et al.*, 2002; Hart *et al.*, 2010; Whitfield *et al.*, 2010). Fluctuations in these synoptic forcings have considerable influence on the major climate parameters driving river discharge, including winter snow accumulation and melt-season temperatures (Moore and McKendry, 1996; Stahl *et al.*, 2006; Stewart, 2009). Late melt-season flows in nival-regime basins are particularly sensitive to changes in these climate conditions as, unlike glacierized systems, they lack the discharge-

moderating influence of glacier ice-melt (Nijssen *et al.*, 2001; Barnett *et al.*, 2005). The attendant vulnerability to multi-decadal climate fluctuations enhances the need to investigate long-term riverflow dynamics in nival systems.

Most large rivers in this region originate from nival basin headwaters located in the rainshadow of the Coast Mountains and drain westward to empty into the Pacific Ocean (Smith, 2001). The low flow regimes that generally distinguish the winter months are related to cold seasonal temperatures and accumulation of the seasonal snowpack. High flows typifying the late spring and summer months characteristically result from melting winter snowpacks that follow warm spring and summer temperatures (Court, 1962; Eaton and Moore, 2010). Sustained declines in the melt-season discharge of these rivers leads to a reduction in the quantity of available freshwater and impacts riparian habitats crucial for many species of fish and animals (Poff and Ward, 1989; MacHutchon *et al.*, 1995; Schindler, 1997, 2001; Wood and Corpé, 2001; Bates *et al.*, 2008).

Hydrometric records for basins located in this region are typically of short-duration and constrain the understanding of hydrologic variations to within the last century. Previous research demonstrates that proxy riverflow records developed using annually resolved tree-ring measurements provide an opportunity to extend instrumental records and assess the long-term dynamics of these river systems (Stockton and Fritts, 1973; Case and MacDonald, 2003; Gedalof *et al.* 2004; Watson and Luckman, 2005; Axelson *et al.*, 2009; Hart *et al.*, 2010). Although prior tree-ring discharge modelling has largely focused on extracting paleorecords from moisture-sensitive trees (Woodhouse *et al.*, 2006; Axelson *et al.*, 2009), recent dendrohydrologic research confirms the value of

also incorporating the climate signals inherent to temperature-sensitive trees. For example, Hart *et al.* (2010) successfully reconstructed a 240-year long discharge history of the Chilko River, draining a glacierized watershed in the central Coast Mountains. Ring-width records from temperature-sensitive Engelmann spruce (*Picea engelmanni*) and temperature- and snowpack-sensitive mountain hemlock (*Tsuga mertensiana*) trees were successfully correlated to develop generalized linear models for mean June, July, and June-July discharge.

The purpose of the research presented in this paper was to develop tree-ring derived insights into the melt-season discharge variability of nival basins in west central British Columbia. While previous dendrohydrologic studies have confirmed that ring-width records can be employed to reconstruct riverflow, this study establishes the benefits of also using temperature-sensitive densitometric records in prehistoric discharge modelling. A secondary goal of this research was to assess the long-term influence of synoptic ocean and atmospheric climate oscillations, summer temperature anomalies and fluctuations in end-of-winter snow water equivalent (SWE) in seasonal snowpacks on variations in melt-season nival river discharge.

2.2 Study Area

Physiographically, the study area encompasses a broad region of west central British Columbia (Figure 2.1). Along the western border of the study area, the rugged peaks of the glaciated Coast Mountains dominate the British Columbia coastline. The high-elevation Chilcotin and Nechako plateaus

characterize the southeast regions of the study area, while the Skeena Mountains distinguish regions to the northeast (Bostock, 1948).

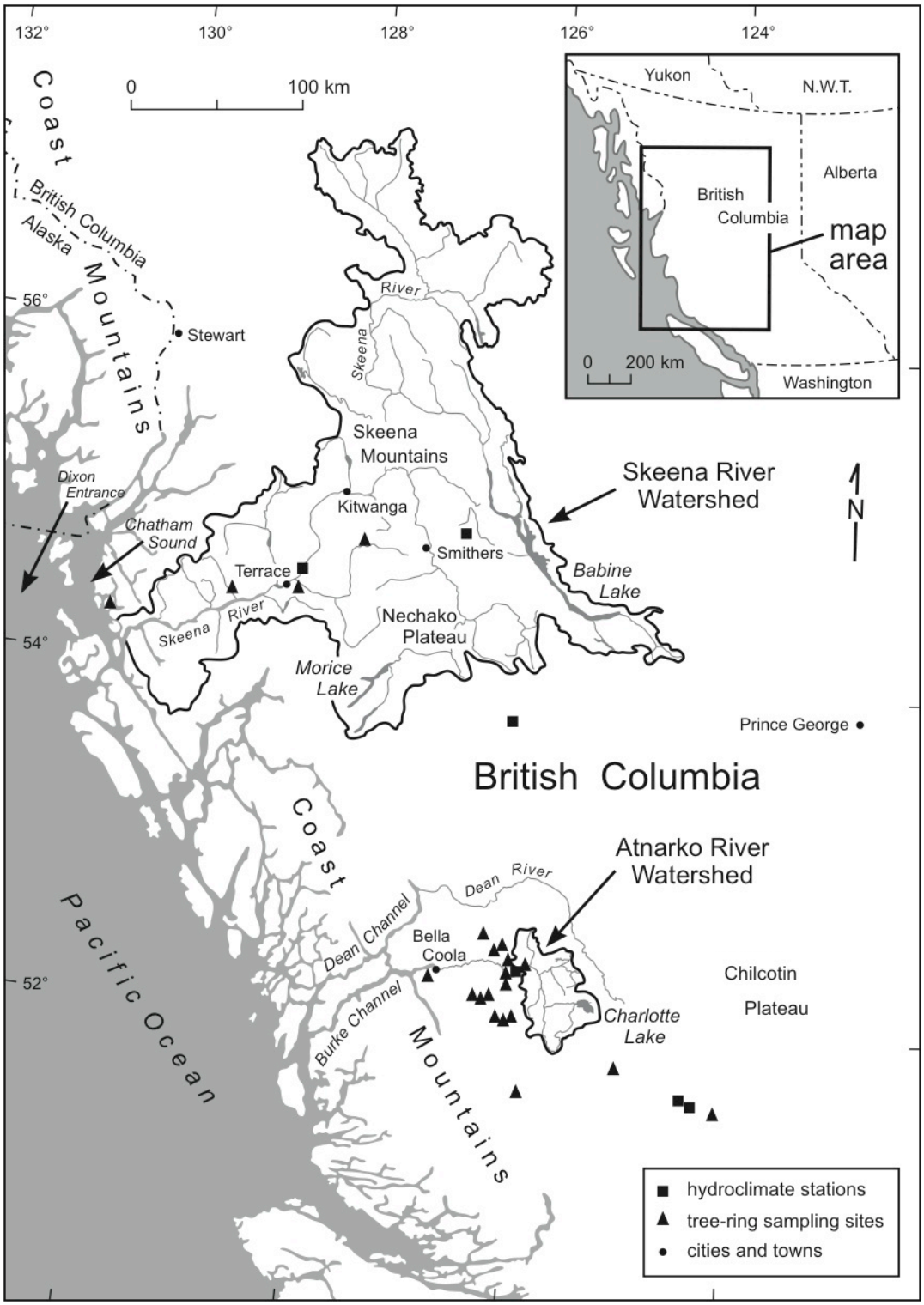

Figure 2.1 Map of west central British Columbia study region

Climates vary with respect to relative proximity to the Pacific Ocean and Coast Mountains (Kendrew and Kerr, 1955; Moore *et al.*, 2010). The western flank of the study area, including the Pacific coastline and windward side of the Coast Mountains, is typified by moderate temperatures and high precipitation totals. Eastern portions are found within the Coast Mountain rainshadow and experience comparatively cooler, drier conditions. These conditions are accentuated to the north within the Skeena River basin.

Coastal regions in the study area are located within the Western and Mountain Hemlock biogeoclimatic zones (Meidinger and Pojar, 1991). Stands of western hemlock (*Tsuga heterophylla*), western redcedar (*Thuja plicata*) and Douglas-fir (*Pseudotsuga menziesii*) characterize low-elevation forests, while stands of mountain hemlock, yellow cedar (*Callitropsis nootkatensis*) and subalpine fir (*Abies lasiocarpa*) distinguish high-elevation landscapes. Eastern regions of the study area are found within the Engelmann Spruce – Subalpine Fir biogeoclimatic zone, where stands of Engelmann spruce, amabilis fir (*Abies amabilis*) and subalpine fir dominate low- and mid-elevation forests. Stands of mountain hemlock, whitebark pine (*Pinus albicaulis*) and subalpine fir characterize higher elevations. Southeastern portions of the study area include representatives of the Montane Spruce and Interior and Coastal Douglas-Fir zones.

Major river systems within the study area are typically nival in regime and originate east of the Coast Mountains (Smith, 2001). The Skeena River basin is the largest in the region covering an area of 54,400 km^2 (WSC, 2010). From its headwaters on the northern interior Nechako Plateau and in the Skeena

Mountains, the Skeena River flows southwest to pass through the Coast Mountains in a broad glacial valley extending from Kitwanga to Dixon Entrance. Babine and Morice lakes distinguish headwater regions, and drain an interior plateau landscape that provides essential riparian and freshwater habitat for transient Pacific salmon populations (Gottesfeld and Rabnett, 2008). Although primarily nival in regime at the Skeena River hydrometric gauging station (Table 2.1), seasonal flows within the basin are augmented by melting glaciers as the river passes through the Coast Mountains (Eaton and Moore, 2010).

Table 2.1 Hydroclimate station locations

Station	Type	ID	Years	Latitude/Longitude	Elevation (m asl)
Tatlayoko Lake	Meteorologic	1088010	1930-2005	51°40'N, 124°24'W	870
Wistaria	Meteorologic	1088970	1926-2004	53°50'N, 126°13'W	863
Tatlayoko Lake	Snow survey	3A13	1964-1998	51°38'N, 124°19'W	1710
Mount Cronin	Snow survey	4B08	1969-2009	54°55'N, 126°48'W	1491
Skeena River	Hydrometric	08EF001	1936-2009	54°38'N, 128°26'W	
Atnarko	Hydrometric	08FB006	1965-2009	52°22'N, 126°00'W	

To the south, the Chilcotin Plateau is drained by comparatively smaller westward flowing basins that include the Bella Coola and Dean rivers. The Atnarko River is a major nival tributary of the Bella Coola River that originates on the Chilcotin Plateau at Charlotte Lake. Draining an area of 2400 km^2 the Atnarko flows westwards to join the glacierized Talchako River and form the Bella Coola River (WSC, 2010).

Over 70% of the total annual discharge for the Skeena and Atnarko rivers occurs during the May-September melt-season (Eaton and Moore, 2010). In contrast, winter season discharge (October-April) is typically low and punctuated

by short-duration extreme flow events resulting from rain or rain-on-snow melt (Court, 1962).

2.3 Methods and Data

A dendrohydroclimatic modelling approach was used to develop long-term discharge records for the Skeena and Atnarko basins. The two rivers have lengthy instrumental flow records and were identified as nival basins representative of those draining the study area.

Tree-ring records were collected from multiple species within a variety of environments to establish a robust regional dataset. These records were correlated to monthly records of hydroclimate (i.e. mean river discharge, mean temperature, total precipitation and SWE) to determine the nature and magnitude of any dendrohydroclimatic relationships. Once the character of these relationships was established the monthly hydroclimate records that correlated strongly to tree-growth were averaged into composite seasonal means and modelled using generalized linear regression. Resultant models demonstrating significant predictive capability were then used to extend instrumental hydrologic records and identify past intervals of anomalously high and low runoff. Supplementary proxy records describing the influence of regional climate conditions (i.e. temperature, precipitation and SWE) and large-scale ocean and atmospheric climate forcings on melt-season discharge were constructed and used to further assess annual discharge regimes within these nival basins.

2.3.1 Hydroclimate and Atmospheric Teleconnection Index Data

Daily mean discharge records for the Atnarko and Skeena rivers were obtained from the Water Survey of Canada website (WSC, 2011) (Table 2.1). Daily records were used to calculate mean monthly and seasonal discharges. Monthly mean temperature and total monthly precipitation records for the Tatlayoko Lake and Wistaria weather stations were retrieved from the Adjusted Homogenized Canadian Climate Database (AHCCD, 2010). April 1 and May 1 snowpack depth and SWE records for Tatlayoko Lake and Mount Cronin were obtained from the British Columbia River Forecast Centre (BC RFC, 2010). Missing values within the hydroclimate records were few and were replaced with long-term averages. Monthly mean atmospheric teleconnection index (ATI) records for the Pacific Decadal Oscillation (PDO) and the Pacific North American pattern (PNA) were obtained from the Joint Institute for the Study of the Atmosphere and Ocean website (JISAO, 2011). Monthly Southern Oscillation Index (SOI) records and NINO 3.4 index records, both measuring variability linked to the El Niño-Southern Oscillation (ENSO), were retrieved from the Australian Bureau of Meteorology (ABM, 2011) and the National Center for Atmospheric Research (NCAR, 2010) websites, respectively.

2.3.2 Tree-Ring Data

Tree-ring records were developed from increment core samples. Sampling for ring-width chronologies involved extracting two 5-mm increment cores from each tree. Cores were collected at 90°-180° from each other close to the tree base. For wood density analysis a third 12-mm core was collected at selected sites

above one of the 5-mm boreholes. Whenever possible the angle and direction of the latter was adjusted to maximize the percentage of perpendicular ring boundaries included within the sample. Additional ring-width samples were extracted from standing dead wood to increase the chronology sample depth during the earliest period of record.

The cores were transported to the University of Victoria Tree-Ring Laboratory and processed using standard procedures (Stokes and Smiley, 1964). After air-drying, the 5-mm samples were glued to slotted boards and sanded to a 600-grit polish. Ring-widths were measured to 0.01 mm using a high-resolution flatbed scanner coupled with WinDendro (Version 2008g) software (Guay *et al.*, 1992).

The 12-mm density cores were air-dried, glued flush to wooden blocks, and cut using a Waltech high-precision twin-bladed saw to produce 2-mm thick wood laths (Haygreen and Bowyer, 1996). Water and resin were extracted from the laths over a period of six hours using an acetone Soxhlet apparatus (Schweingruber *et al.*, 1978; Jensen, 2007). The laths were then x-rayed for 20 μs at 50-μm intervals using a digital ITRAX scanning densitometer equipped with a Chromium x-ray tube set to maintain 30 mA and 55 kV of power. Ring-width and maximum wood density values were measured from each digital x-ray image using WinDendro (Version 2008g) software.

Unusually narrow rings in the ring-width series were identified and used as marker years to visually cross-date each chronology (Stokes and Smiley, 1964). The quality of the visual cross-dating was independently verified using COFECHA (Holmes *et al.*, 1986). Cross-dating correlations were calculated for

50-year segments with a 25-year lag and considered significant at the 0.01 level (Grissino-Mayer, 2001). The density chronology was visually cross-dated and verified using the corresponding ring-width measurements. To ensure that a common signal was captured, individual series not significantly correlating to the master series were removed. Following this procedure, the cross-dated ring-width chronologies were combined into regional species-specific chronologies.

The cross-dated regional chronologies were standardized using ARSTAN by double-detrending each series (Holmes *et al.*, 1986). Age-growth related trends were removed by fitting a negative exponential curve or a linear regression line through the mean of each series (Fritts, 1976). A second conservative detrending was completed to reduce non-climatic influences on ring growth using a cubic smoothing spline with a 67% frequency-response cutoff. This ensured that 50% of the variance in ring growth was retained at a frequency of two-thirds the series length (Cook, 1985). After detrending the tree-ring data, standardized master chronologies were constructed using a robust biweighted mean to enhance the common signal found between all series (Cook, 1985). Residual chronologies were also constructed by removing the low-order autocorrelation from the standardized data, thus limiting the influence that growth from the previous year has on the current growth year (Cook and Krusic, 2005). Both standardized and residual chronologies were used in this study. Expressed population signal (EPS) values were calculated to quantify the signal strength and identify periods where the chronology variability was distorted by decreased sample depth (Wigley *et al.*, 1984; Cook and Krusic, 2005). Master chronologies

with multiple distinct stand-age cohorts were reduced in sample depth to include only long-lived trees.

2.3.3 Dendrohydroclimate Correlations and Reconstructions

Correlations were calculated between monthly records of river discharge, master tree-ring chronologies, climate variables and ATIs. All monthly hydroclimate records from the current and previous years, with the exception of October-December records for the current growth year, were used in the dendrohydroclimate correlation analyses. Correlations were considered statistically significant at the 0.05 level.

Monthly discharge records strongly correlated to tree growth and climate variables were averaged into composite seasonal mean runoff records and were modelled using generalized linear regression. Master tree-ring chronologies demonstrating strong correlative relationships to the discharge records were considered as predictor variables in the regression models. All possible combinations of the selected predictor variables were developed into a series of candidate tree-ring models and were compared using correlation coefficient (R) statistics. The candidate model demonstrating the strongest R was identified and subjected to further model quality testing prior to reconstructing discharge records. Select climate records strongly related to tree growth and discharge were similarly reconstructed to provide a robust examination of the prehistorical hydroclimate of west central British Columbia.

The tree-ring models were independently verified using the leave-one-out method to allow for calibration over the duration of the instrumental record

(Gordon, 1982). Individual linear regression models were constructed for each year of the instrumental record in question. Each model had a different datum year removed prior to model calibration and was subsequently used to predict the missing value. The predictive capacity of each model was evaluated by correlating instrumental records with the predicted records obtained during the leave-one-out process. Coefficient of variation (R^2) statistics calculated for each reconstruction provided a measure of the instrumental variability explained by tree-ring models. Reduction of error (RE) statistics yielded a secondary evaluation of model quality (Fritts, 1976; Hart *et al.*, 2010). Models demonstrating positive RE statistics, strong R^2 values and significant correlations between instrumental and predicted records were deemed adequate for extending hydroclimate records.

Tree-ring reconstructed hydroclimate records were standardized into deviations from the instrumental record average. This procedure generated records of hydroclimate anomalies and allowed for comparisons between all proxy records presented in the study. Notable periods of record displaying persistent variability either above or below the long-term instrumental mean were identified.

Long-term relationships to ocean and atmospheric climate forcings were identified using correlation and wavelet analyses. Initially, correlations were calculated between the winter season (October-April) mean values for SOI, NINO 3.4, PDO and PNA indices and the reconstructed hydroclimate records. Additional long-term assessments were completed by correlating the extended hydroclimate records to tree-ring derived proxy indices of the PDO and the PNA.

Wavelet analysis using a Gaussian 2 function coupled with a 5% red-noise reduction was used to identify the frequency of any cyclical patterns within the proxy hydroclimate records (http://www.paos.colorado.edu/research/wavelets; Torrence and Compo, 1998).

2.4 Results

2.4.1 Tree-Ring Chronologies

Tree-ring sampling was conducted at 18 sites between 1997 to 2010 within the Coast Mountains and adjacent plateau areas of west central British Columbia (Figure 2.1, Table 2.2). Increment cores were collected from mature mountain hemlock (MH), Douglas-fir (DF), subalpine fir (SF), whitebark pine (WBP) and yellow cedar (YC) trees.

Table 2.2 Tree-ring chronology sampling locations

Sampling Site	ID	Species	Data	Sampled	Latitude/Longitude	Elevation (m asl)
Cable Spur	CBS	mh	w	2005	54°50' N, 127°48' W	1090
Copper Mountain	CU	mh	w	2005	54°30' N, 128°28' W	887
Clayton Falls	CFY	yc	w	2010	52°17' N, 126°53' W	874
Exstew River	EXR	mh	w	2005	54°29' N, 129°07' W	875
Fisheries Pool	FSH	df	w	2010	52°23' N, 126°05' W	192
Hammer Lake	SWP	sf	w	2010	52°12' N, 126°19' W	1291
Jacobson G.	DDA	sf	w	2010	52°04' N, 126°08' W	1477
	DDd	sf	d	2010	52°04' N, 126°08' W	1477
	JCB	wbp	w	2010	52°04' N, 126°09' W	1469
Liberty Glacier	LIB	wbp	w	2001	51°35' N, 124°05' W	1525
Mount Hayes	HAY	mh	w	2005	54°17' N, 130°19' W	665
Noosgultch Creek	NS	df	w	1997	52°27' N, 126°06' W	250
Nordshow Creek	NRD	df	w	1997	52°18' N, 126°06' W	650
Nusatsum Pass	NUS	mh	w	2010	52°13' N, 126°20' W	1079
	NM	mh	w	1997	52°14' N, 126°19' W	1035
Perkin's Peak	PRK	wbp	w	2010	51°50' N, 125°03' W	1960
Siva G.	SV	wbp	w	2001	51°39' N, 125°55' W	1500
Tweedsmuir	TWD	df	w	1997	52°24' N, 125°55' W	300
Tzeetsaytsul G.	TZ	sf	w	1997	52°35' N, 126°22' W	1260
Valley View High	VH	df	w	1997	52°28' N, 126°13' W	1270
Valley View Low	VL	df	w	1997	52°26' N, 126°12' W	650

df – Douglas-fir, mh – mountain hemlock, sf – subalpine fir, wbp – whitebark pine, yc – yellow cedar, G – glacier, w – width, d – density

MH sampling took place at five high-elevation sites in the Coast Mountains within homogenous to mixed stands that included SF and western hemlock (WH) cohorts. DF samples were collected at six sites within homogenous valley bottom to high-elevation stands in the Bella Coola River Valley. SF sampling occurred at three high-elevation Coast Mountain locations within cohabitating stands of MH, WBP and/or WH. WBP samples were collected at four high-elevation sites within homogeneous to mixed cohort stands located in both the Coast Mountains and Chilcotin Plateau. YC sampling occurred within a mixed stand of SF and WH on a high-elevation northeast-facing Coast Mountain slope.

The extensive number of tree-ring samples collected from different tree species in a variety of environments is assumed to constitute a high-quality regional representation of tree growth within west central British Columbia. The multi-species tree-ring network contains 21 site-specific chronologies ranging from 975-269 years in length. Ring-width measurements for the MH, DF, SF and WBP were combined into four regional species-specific master chronologies (Figure 2.2, Table 2.3). The YC ring-width and SF maximum ring-density (SFd) chronologies remain single-site species-specific master chronologies. Tree ages in the YC and DF master chronologies indicate the presence of two distinct age groups within sampled stands. Cores younger than 500 years in the YC chronology and 300 years in the DF regional chronology were removed to create lengthy master chronologies from a single age cohort.

Table 2.3 Summary statistics for individual and regional tree-ring chronologies

ID	Species	Data	Range (yrs AD)	# cores	# years	Interseries Correlation	Mean Sensitivity
SWP	sf	w	1727-2009	51	283	0.550	0.198
DDA	sf	w	1533-2009	67	477	0.566	0.192
TZ	sf	w	1729-1997	25	269	0.525	0.190
JCB	wbp	w	1139-2009	81	871	0.545	0.191
PRK	wbp	w	1449-2009	40	561	0.513	0.214
LIB	wbp	w	1637-2000	31	364	0.492	0.185
SV	wbp	w	1531-2000	34	470	0.547	0.218
CBS	mh	w	1616-2004	33	389	0.615	0.203
CU	mh	w	1646-2004	41	359	0.676	0.261
EXR	mh	w	1576-2004	30	429	0.607	0.245
HAY	mh	w	1556-2004	20	449	0.618	0.260
NUS	mh	w	1638-2009	49	373	0.604	0.226
NM	mh	w	1712-1996	33	285	0.485	0.217
FSH	df	w	1592-2009	54	418	0.512	0.177
NS	df	w	1624-1996	15	373	0.560	0.228
NRD	df	w	1400-1996	29	597	0.505	0.188
VH	df	w	1692-1996	22	305	0.564	0.234
VL	df	w	1625-1996	17	372	0.600	0.261
TWD	df	w	1554-1996	16	443	0.476	0.198
DF*	df	w	1400-2009	56	610	0.471	0.192
MH*	mh	w	1556-2009	210	455	0.524	0.234
SF*	sf	w	1533-2009	143	477	0.518	0.194
SFd	sf	d	1636-2009	27	375	0.475	0.059
WBP*	wbp	w	1139-2009	186	871	0.450	0.202
YC	yc	w	1035-2009	27	975	0.586	0.237

Chronologies in the shaded region are the six species-specific master chronologies.
Chronologies denoted with a * are species-specific regional chronologies.
w – width, d – density

2.4.2 Hydroclimate Correlations within the Instrumental Record

Correlation analyses revealed strong relationships among summer air temperature, end-of-winter SWE and summer river discharge. Late melt-season (July-August) mean discharge records for the Atnarko and Skeena rivers most strongly correlated to May 1 SWE measurements at Mount Cronin (Atnarko, r = 0.701; Skeena, r = 0.629) and Tatlayoko Lake (Atnarko, r = 0.640; Skeena, r=0.339). Significant negative correlations were observed between July-August mean discharge and summer (June-August) mean air temperature recorded at Tatlayoko Lake (Atnarko, r = -0.532; Skeena, r = -0.620) and Wistaria (Atnarko, r = -0.443; Skeena, r = -0.685).

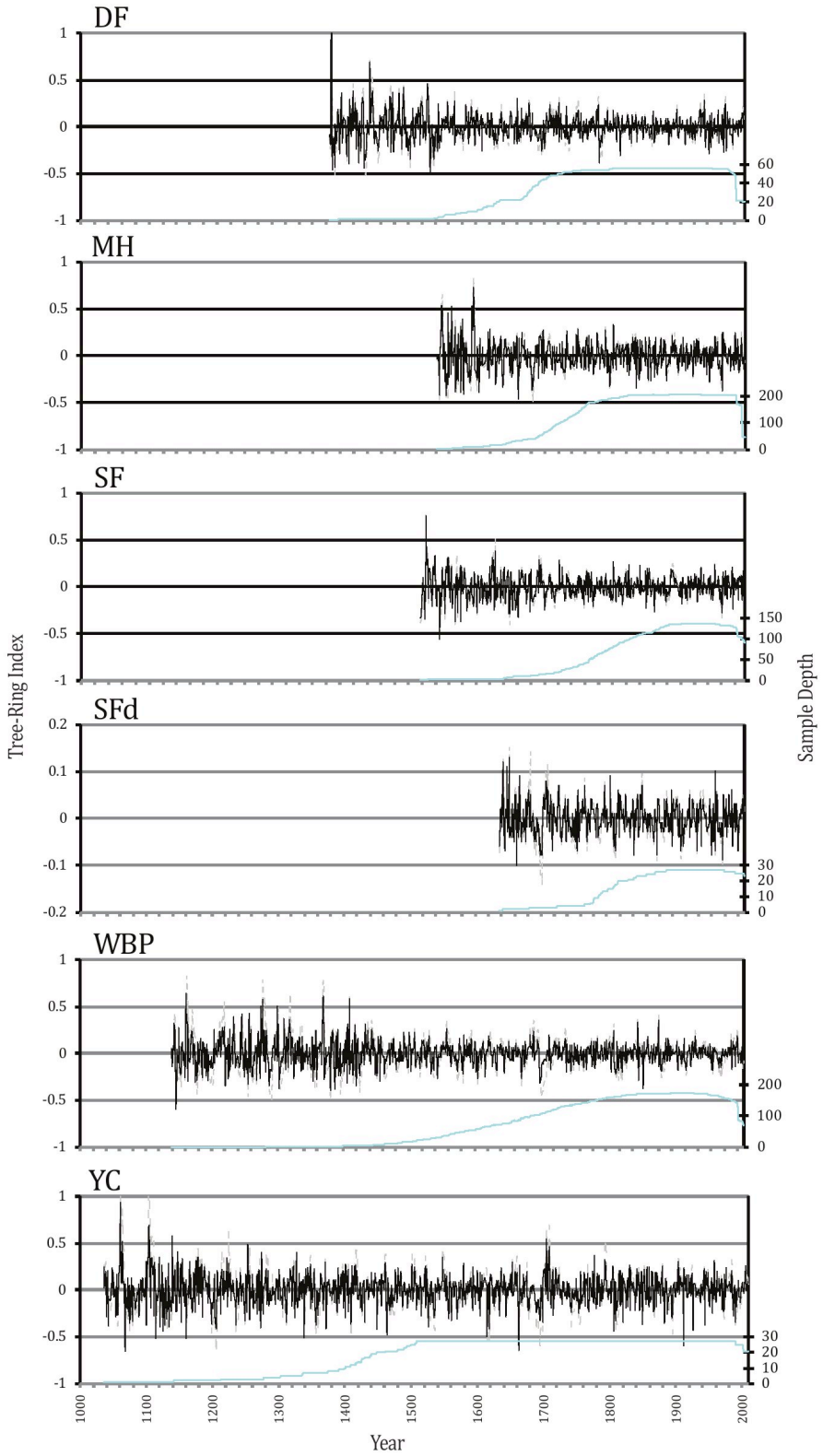

Figure 2.2 Standardized and residual master tree-ring indices. Solid black lines represent standardized data, dashed gray lines represent residual data. Blue line indicates sample depth.

2.4.3 Dendrohydroclimate Correlations

Significant correlations were detected between the standardized and residual tree-ring chronologies and all selected hydroclimate variables (Figure 2.3). With the exception of most correlations to the ATIs, the standardized chronologies generally exhibited marginally stronger correlations to the hydroclimate records. Although strong significant correlations were often shown by both standardized and residual chronologies reported correlations were only provided for the master chronology demonstrating the strongest relationship to monthly hydroclimate records.

Significant negative correlations exist between the standardized chronologies and the melt-season discharge records for the Skeena and Atnarko rivers during the year of tree-ring growth. The strongest of these correlations were to SF, SFd, MH and WBP chronologies. WBP also correlated strongly to the late melt-season (July-August) discharge records from the previous year.

Significant correlations with mean monthly temperature during the winter season (October-April) preceding growth and the current summer season (June-August) were positive for all tree species. In contrast, significant negative correlations to prior summer temperatures and end-of-winter SWE were recorded. Weak significant correlations were identified between precipitation records and tree-ring chronologies. The strongest of these correlations was detected between total previous November precipitation and the SF chronology ($r = -0.372$). The majority of the remaining significant correlations with monthly precipitation records were detected between ring growth and previous summer precipitation.

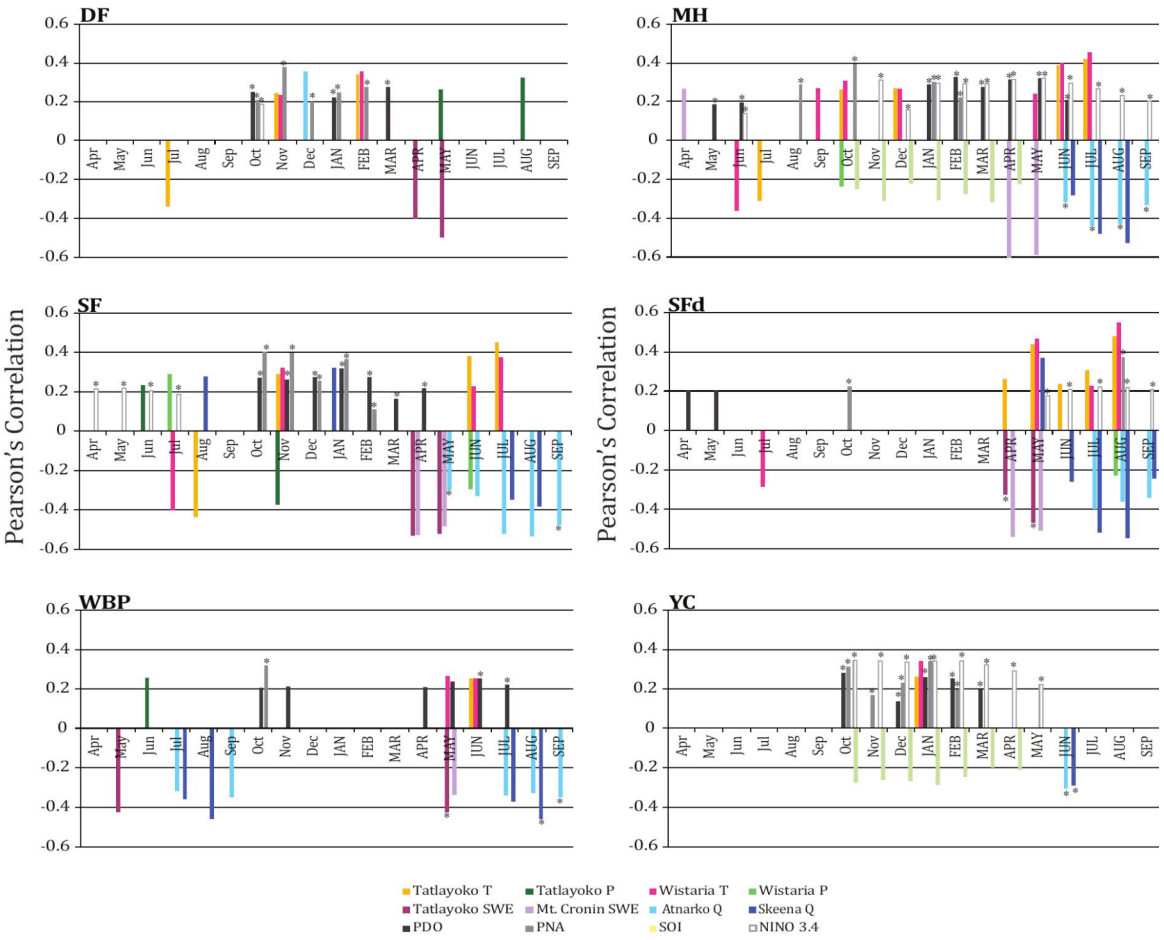

Figure 2.3 Significant Pearson's correlation coefficients between master tree-ring chronologies and monthly hydroclimate records ($p \leq 0.05$). All months in lower case letters represent months from the year preceding growth. Where both standardized and residual chronologies significantly correlate to records only the strongest relationship is reported. Correlations marked by * are calculated using residual chronologies.

Significant correlations were present between residual tree-ring chronologies and all ATIs (Figure 2.3). Correlations were typically positive between chronologies and the NINO 3.4, the PDO and the PNA indices. Generally negative correlations were noted to the SOI. The strongest and most significant relationships exist between residual chronologies and winter (October-February) PNA.

2.4.4 Hydroclimate Reconstructions

The strong correlations detected between hydroclimate records and tree-ring chronologies provided a sound basis for dendrohydroclimatic reconstructive modelling. Proxy records of July-August mean discharge were constructed for the Skeena and Atnarko rivers. Five supplementary climate and ATI records were also reconstructed to document their relationship to river discharge trends. These include June-August mean temperature for Tatlayoko Lake and Wistaria, May 1 SWE at Tatlayoko Lake and Mount Cronin and October-February mean PNA. All tree species were utilized in at least one of seven hydroclimate models constructed.

All reconstructions demonstrate significant predictive capabilities, verified by both positive RE statistics and strong R^2 statistics (Table 2.4). Visualization of the calibration period for the Atnarko River proxy record highlights the tendency for the model to underestimate the magnitude of discharge anomalies (Figure 2.4). This underestimation is responsible for some of the unexplained instrumental variability not captured by the tree-ring proxy record and indicates that the magnitude of predicted extreme low flow events may be modest in scale. The Skeena River discharge model is more proficient at capturing the magnitude of runoff anomalies, although a significant overestimation was detected during the mid-1960s. Visualizations of the calibration period for the accompanying climate reconstructions are available in Appendix A. Reconstructions of composite hydroclimate variables such as end-of-winter SWE, summer discharge and the PNA were generally more robust than proxy records of individual climate variables. This observation reflects the complexities associated with

reconstructing individual hydroclimate variables using trees that have a tendency to react to and record multiple climate signals (Smith and Laroque, 1998; Peterson *et al.*, 2002; Woodhouse, 2003; Grossnickle and Russell, 2006; Griesbauer *et al.*, 2011).

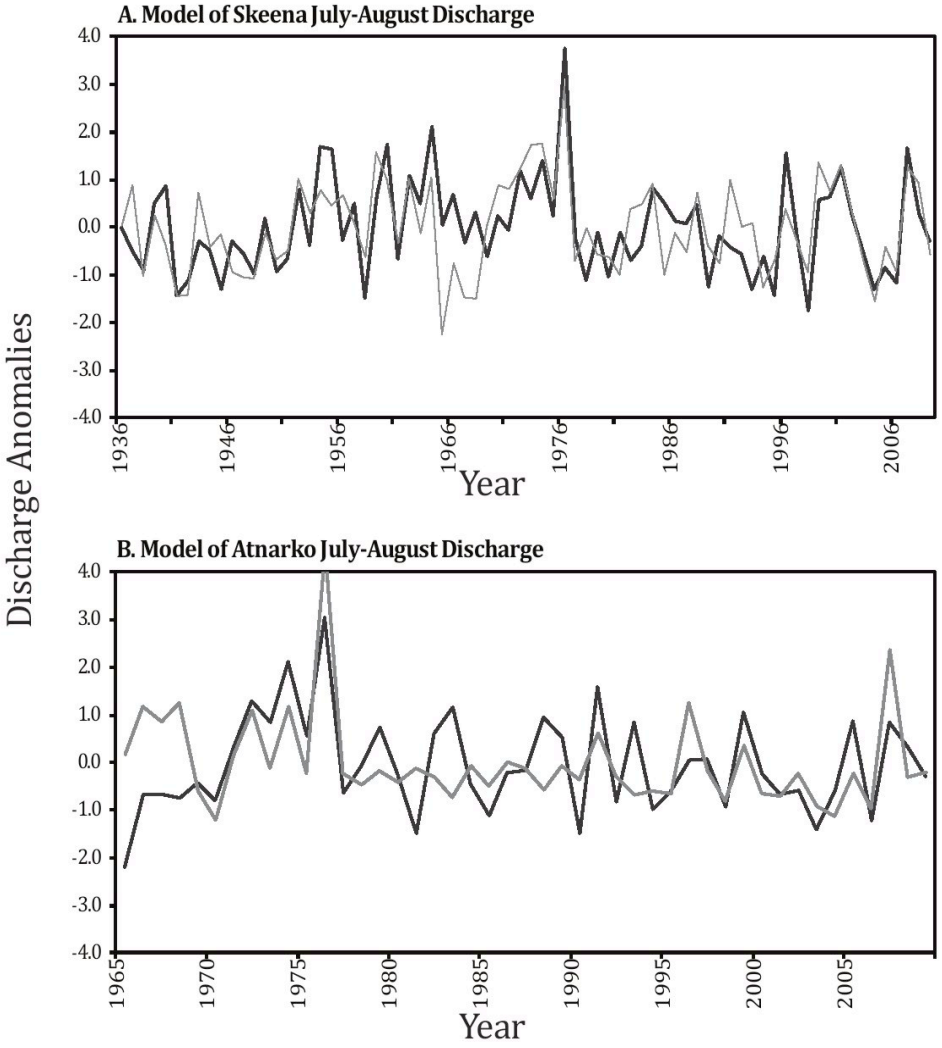

Figure 2.4 Comparison between reconstructed (black line) and instrumental (gray line) records of July-August mean runoff for the Skeena and Atnarko rivers during the calibration period.

Table 2.4 Summary statistics for hydroclimate reconstructions

Hydroclimate Variable	R	Rv	R^2	RE	Chronologies	Proxy Duration	EPS[1]
Tatlayoko May 1 SWE	0.65	0.55	0.43	0.50	SF, DF	1533-2009	1660
Mt Cronin May 1 SWE	0.64	0.51	0.42	0.43	SFd, WBP, MH	1636-2009	1790
Tatlayoko June-Aug T	0.51	0.46	0.26	0.27	SF, MH	1556-2009	1660
Wistaria June-Aug T	0.56	0.51	0.31	0.37	SFd, MH	1636-2009	1790
PNA Oct-Feb	0.61	0.54	0.37	0.41	DF*, SF*, YC*	1533-2009	1660
Atnarko July-Aug Q	0.55	0.50	0.30	0.29	SF, MH*	1533-2009	1660
Skeena July-Aug Q	0.66	0.62	0.44	0.41	SFd, MH	1660-2009	1790

[1]Date that a decrease in sample depth drops the EPS for one chronology below 0.85
Rv – Correlation coefficient statistics for verification period, T – temperature, Q – discharge,
* – residual chronology

The reconstructed proxy records of July-August discharge for the Atnarko and Skeena rivers respectively explain 28-44% of the variability over the instrumental period. The strength of the Skeena basin reconstruction is a significant improvement over results from previous tree-ring derived proxy records of discharge in western Canada (e.g. Gedalof *et al.*, 2004; Watson and Luckman, 2005; Hart *et al.*, 2010). Reconstructions of selected climate variables explain between 26-43% of the variation in their respective instrumental records (Table 2.4).

Recognizing the strength of the tree-ring proxy models presented in this paper, anomalies for the seven hydroclimate variables were reconstructed back to 1660 AD (Figure 2.5). Variability in reconstructions of Skeena River discharge, Wistaria temperature and Mount Cronin SWE were influenced by decreased sample depth in the SFd chronology before 1790 AD. However, the general agreement between all reconstructions, regardless of sample depth provides rationale for including these reconstructions back to 1660 AD.

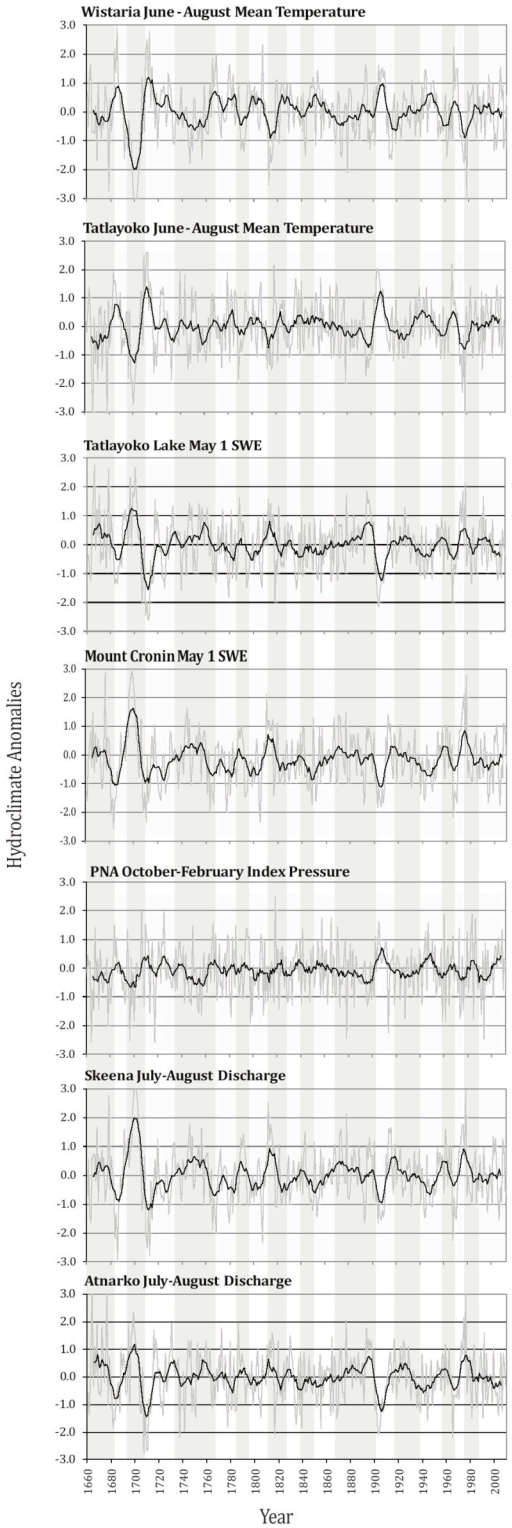

Figure 2.5 Reconstructions of west central British Columbia hydroclimate anomalies from 1660 AD to present. Gray lines are the actual reconstructions while the black lines represent a 10-year running mean of the data. Shaded gray areas illustrate intervals typically exhibiting above average July-August runoff.

2.5 Discussion

2.5.1 Hydroclimate Correlations within the Instrumental Record

The positive correlations between end-of-winter SWE and late melt-season discharge reflect the amount of freshwater contributed by the seasonal snowpack (Moore, 1996). The negative correlations between summer temperature and late melt-season discharge likely reflect the overall negative relationship between the annual and winter mean temperatures and melt-season discharge. Previous hydroclimatic research typically finds the relationship between discharge and summer temperature to be positive, reflecting the increase in stream discharge that accompanies temperature-dependent snowmelt (Whitfield, 2001; Hart *et al.*, 2010). However, warmer winter and annual temperatures are associated with a lower than average end-of-winter snowpack (Stahl *et al.*, 2006) resulting in a reduction of the seasonal freshwater store available for melt during the summer months. The significant positive correlations present between summer (June-August) and annual mean temperatures at Wistaria (r =0.498) and Tatlayoko Lake (r =0.385) coupled with the negative correlations found between annual mean temperature and July-August discharge for the Skeena (Tatlayoko Lake, r = -0.284; Wistaria, r =-0.370) and Atnarko (Tatlayoko Lake, r =-0.209; Wistaria, r =-0.274) rivers provide evidence to support this assessment.

An additional hypothesis that may explain the negative relationship between discharge and summer temperature is the role of evapotranspiration on decreasing melt-season water availability (Hamlet *et al.*, 2007). The absence of lengthy evapotranspiration data within west central British Columbia prevented further investigations into this relationship. Regardless, the inclusion of

evapotranspiration variables in future dendrohydrologic research may offer additional insights on long-term nival river discharge.

2.5.2 Dendrohydroclimate Correlations

Like the runoff records, radial tree growth measurements strongly correlate to variations in summer temperature and end-of-winter SWE, indicating that corresponding signals from both climate parameters were contained within the riverflow and tree-ring records. The strong correlative relationship between tree growth and discharge supports this conclusion. Recognizing this interconnectedness, it was postulated that the physiological relationship between tree-ring growth and climate provides a useful proxy for interpreting the relationship between the climate-integrated variables of tree-ring growth and melt-season river discharge.

Dendroclimatic research has established the physiological connections between tree-ring growth and fluctuations in end-of-winter SWE and summer temperatures. The significant negative correlations detected between SWE and tree-ring chronologies in this study likely reflect the persistence of the end-of-winter snowpack associated with above average SWE years. Late-melting end-of-winter snowpacks maintain near-freezing temperatures in soil late into the spring and early summer, delaying the initiation of the growth season and bud development (Gedalof and Smith, 2001b; Peterson and Peterson, 2001; Laroque, 2002; Peterson *et al.*, 2002). Thus, a winter with above average SWE is indicative of both increased melt-season discharge and depressed ring growth.

The positive correlations present between tree-ring measurements and summer temperature reflect the increased cone production, earlier bud and needle maturation and enhanced photosynthesis associated with increased ring-width and warmer temperatures (Peterson *et al.*, 1990; Woodward et al., 1994; Peterson and Peterson, 2001; Peterson *et al.*, 2002; Grossnickle and Russell, 2006; Griesbauer *et al.*, 2011). As the tree-ring growing season is typically completed by mid-summer (Laroque and Smith, 2003), correlations between ring-width and August temperature are likely caused by persistent weather conditions producing warmer or cooler temperatures through the entire summer period. Increased late spring and early summer temperatures also promote an earlier initiation of cambial activity, which is shown to benefit the cell-wall thickening process connected to wood density during the later summer (July-August) period (D'Arrigo *et al.*, 1992; Splechtna *et al.*, 2000; Davi *et al.*, 2002).

Similar to correlations between tree growth and discharge, the correlations detected between tree growth and October-February PNA reflect the changes in climate conditions typically associated with PNA pressure anomalies. Positive (negative) PNA anomalies are associated with a stronger (weaker) Aleutian Low pressure centre and a northward shift (no significant shift) in the usual winter storm track, leading to warmer (cooler) winter temperatures and a decrease (increase) in winter precipitation for central British Columbia (Bonsal *et al.*, 2001; Stahl *et al.*, 2006). Consequently, above average winter PNA provides an indirect and integrated measure of climate conditions and is associated with enhanced ring growth and below average melt-season discharge.

2.5.3 Hydroclimate Reconstructions

Common patterns of variability are present between discharge reconstructions and proxy records of climate, demonstrating the strong regional similarities between sites within west central British Columbia. Collectively, hydroclimatic reconstructions describe intervals of increasing or higher than average July-August runoff totals during periods characterized by cooler summer temperatures, above average snow accumulation and negative winter PNA conditions. Episodes of lower than average discharge occurred during periods distinguished by warmer than average summer temperatures, lower than average end-of-winter snowpacks and typically positive winter PNA pressure anomalies.

The mid- to late-1600s were generally characterized by above average July-August discharge (Figure 2.5). This persistent pattern of runoff was punctuated by a brief episode of decreased discharge in the 1680s. Overall cooler and wetter conditions synchronous with enhanced runoff during the late-1600s may be partially responsible for precipitating a widely recognized interval of glacial expansion during the early- and mid-1700s (Luckman, 2003; Watson and Luckman, 2004; Larocque and Smith, 2005b; Koehler and Smith, 2011). This interval of enhanced melt-season discharge was abruptly replaced by an interval of below average discharge during the early-1700s.

The reconstructions suggest the mid- and late-1700s were characterized by larger than normal runoff, except during the 1760s-1780s when lower than average discharges were recorded. The early-1800s were characterized by decreased melt-season runoff, punctuated by years of higher than normal discharge. The mid-1800s were distinguished by an extended interval of

generally increasing and above average melt-season runoff that persisted until the end of the century. The early portion of the 20th Century was characterized by an abrupt shift to below average runoff that persisted until just before the 1920s, when an interval of larger than average seasonal runoff years began. The remainder of the proxy records describing 20th Century runoff trends are characterized by low-frequency fluctuations in general synchroneity with shifts identified within instrumental records.

2.5.4 Connections to Large-Scale Ocean and Atmospheric Forcings

The long-term proxy records of July-August discharge presented in this paper are characterized by cyclic intervals of above and below average runoff. The persistence of these low-frequency trends suggests that ocean-atmospheric teleconnections have influenced the runoff regimes of the Atnarko and Skeena rivers for the past three and a half centuries. Over the historical period, runoff records for the Atnarko and Skeena rivers show stronger correlations to the PNA and PDO indices than to the SOI and NINO 3.4 index (Table 2.5). Correlations between river discharge and the PDO and PNA are typically negative with episodes of enhanced July-August discharge commonly distinguishing cool PDO phases and periods with generally negative PNA anomalies. Similarly, enhanced July-August runoff is typically associated with La Niña events, represented by years with anomalously positive SOI and negative NINO 3.4 records. Extending the correlation analyses into the pre-instrumental period using proxy reconstructions of spring PDO (Gedalof and Smith, 2001a) and winter PNA (this

study) confirm the persistence of these relationships between discharge and ocean-atmospheric forcings (Table 2.5).

Table 2.5 Correlations between reconstruction records and ATIs

Reconstructed Variables	SOI	NINO 3.4	PDO	PNA	Proxy PDO[1]	Proxy PNA[2]
Tatlayoko May 1 SWE			-0.310	-0.424	-0.331	-0.769
Mt Cronin May 1 SWE	0.243	-0.261	-0.344		-0.499	-0.547
Tatlayoko June-Aug T	-0.201	0.232	0.360	0.353	0.432	0.706
Wistaria June-Aug T	-0.194	0.217	0.306		0.445	0.512
PNA Oct-Feb	-0.223	0.243	0.383	0.549	0.284	
Atnarko July-Aug Q		-0.193	-0.338	-0.346	-0.381	-0.698
Skeena July-Aug Q	0.189	-0.221	-0.268		-0.304	-0.435

[1]Proxy spring PDO (March-May), Gedalof and Smith, 2001a
[2]Proxy winter PNA (October-February), this study
Only correlation results statistically significant at the 0.05 level shown
T – temperature, Q – discharge

Wavelet analysis results concur with those from the correlation analyses, revealing both high- and low-frequency variability in proxy records of river discharge (Figure 2.6). Wavelet results for the climate reconstructions are presented in Appendix B. A higher-frequency (approximately 10-12 year) pattern of variability is detected in all hydroclimate records and may represent climate activity linked with the ENSO. Records also demonstrate a multi-decadal (approximately 20-50 year) mode of variability that may reflect changes in the ocean-atmospheric forcings described by the PDO and PNA indices. This low-frequency signal is most prominent during the late-1600s, early-1700s and the 1900s while notably depressed during the mid- to late-1800s. Findings from prior wavelet analyses on independent tree-ring and sediment proxy reconstructions of hydroclimate throughout western and northern Canada corroborate with results from this study (Gedalof and Smith, 2001a; Lamoureaux

et al., 2006; Kaufman, 2008; Hart *et al.*, 2010). Coupled with the results from the correlation analyses, these findings confirm that the ocean-atmospheric forcings described by the PDO and PNA indices have strongly influenced west central British Columbia discharge dynamics over the past 350 years.

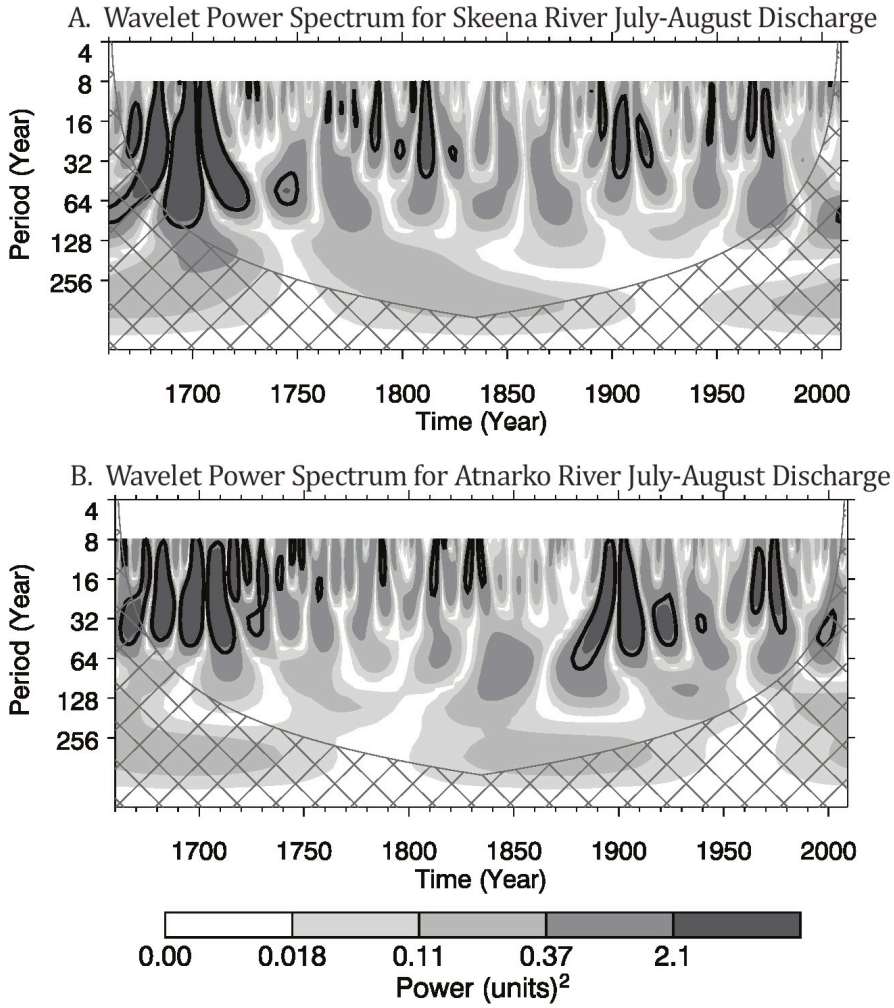

Figure 2.6 Wavelet power spectrum for the Skeena and Atnarko runoff reconstructions. The wavelet power spectrum uses a Gaussian-2 function. Cross-hatched regions of the wavelet diagrams represent the cone of influence where zero-padding of the data was used to reduce variance. Black contours indicate significant modes of variance with a 5% significance level using an autoregressive lag-1 red noise background spectrum (Torrence and Compo, 1998)

2.5.5 Comparisons to Other Paleohydroclimate Records

Anomalies in proxy runoff for the Skeena and Atnarko rivers generally match those found within the 250-year paleorecord of June-July discharge for the glacierized Chilko River (Hart *et al.*, 2010). Periods of above average discharge during the early- and late-1800s were identified in all three reconstructions while comparable episodes of below average summer discharge were described during the mid-1800s and the mid- and late-1900s. The Skeena and Atnarko reconstructions further revealed previously unknown episodes of severe low flow in western British Columbia during the late-1600s and early- and mid-1700s.

Comparisons to other proxy hydrologic records in western Canada increase the fidelity of results presented in this paper. Tree-ring scar derived records of late spring and summer flood events from 1880-1990 in a headwaters tributary of the Skeena basin generally correspond with years distinguished by above average river discharge (Gottesfeld and Johnson Gottesfeld, 1990). Similar parallels extend to regions of the Canadian Rocky Mountains and Canadian prairies, where drought or low flow events in the South Saskatchewan, Oldman (Axelson *et al.*, 2009) and Bow River basins (Watson and Luckman, 2005) generally occur during periods of low flow and diminished end-of-winter SWE in west central British Columbia.

Further similarities are detected with synthesized records of cumulative snowfall (Perkins and Sims, 1983), PDO and annual riverflow (Lamoureux *et al.*, 2006; Kaufman, 2008) derived using varved lake sediment thickness measurements from northern Canada and Alaska. In accordance with

instrumental records (Moore and McKendry, 1996; Bitz and Battisti, 1999; Mantua *et al.*, 1997), periods of reduced cumulative snowfall, low riverflow and negative PDO in northern Canada and Alaska are predicted during periods of above average riverflow and end-of-winter SWE in west central British Columbia. The agreement between tree-ring and varved lake sediment proxy records is particularly encouraging as the lake sediment records provide an entirely independent verification of paleoenvironmental reconstruction.

Extended connections to proxy records of glacier mass balance and glacier advance further reinforce findings presented in this paper. Similar to nival-regime basin discharge, fluctuations in glacier mass balance are known to integrate signals from variations in summer and winter temperatures and end-of-winter snow accumulation (Raper *et al.*, 1996; Larocque and Smith, 2005b). Mass balance reconstructions for glaciers in the southern Coast Mountains and Canadian Rocky Mountains suggest that episodes of positive mass balance and glacier advances distinguished the early- to mid-1700s, the early- and late-1800s and the 1970s (Watson and Luckman, 2004; Larocque and Smith, 2005b). Generally these periods of positive mass balance are analogous with or subsequent to intervals of enhanced end-of-winter SWE and summer discharge in west central British Columbia.

2.6 Conclusion

The two dendrohydrologic reconstructions presented in this paper are the first tree-ring proxy records of nival-regime river discharge in British Columbia. The reconstructions provide an opportunity to evaluate the long-term variability

of melt-season runoff for nival basins throughout west central British Columbia. Analysis of both reconstructed discharge records highlight common intervals of significantly below and above average riverflow throughout the past 350 years. Coupling discharge reconstructions with proxies for June-August mean temperature, end-of-winter SWE and winter PNA provides a more detailed picture of the long-term drivers of runoff dynamics. Episodes of increased July-August discharge are typically associated with increased end-of-winter SWE, cooler mean summer temperatures and negative PNA conditions.

The proxy records for Skeena River July-August discharge and Mount Cronin May 1 SWE are among the first dendrohydroclimatic reconstructions to utilize measures of wood density in Pacific North America. An additional temperature reconstruction using maximum ring density measurements is presented for Wistaria. Comparisons of model statistics between reconstructions solely containing ring-width chronologies and those integrating wood density and ring-width chronologies demonstrate the benefits of including maximum ring-density measurements in hydroclimatic reconstructions.

The findings presented in this paper confirm the significant influence of low-frequency ocean and atmospheric circulation patterns on prehistorical hydroclimatic variability and emphasize the need to improve our understanding of long-term discharge dynamics in British Columbia. The continued retreat and thinning of alpine glaciers will place increasing reliance on seasonal snowpacks and nival-regime watersheds to provide essential freshwater resources to many areas of British Columbia. The prolonged episodes of below average riverflow in both the Skeena and Atnarko basins during the 18th and 19th centuries appear

more severe than events recorded within the instrumental record and demonstrate the immense range of natural riverflow conditions in many nival-regime systems. The possibility of future low flow events of this magnitude should be given proper consideration when building and reassessing water resource management plans.

Chapter 3

Regional scale reconstructions of Pacific salmon abundance for west central British Columbia using climate-sensitive tree-ring records

3.1 Introduction

Historical monitoring of Pacific salmon (*Oncorhynchus* spp.) stocks over the last century reveal marked shifts in their abundance (Mantua *et al.*, 1997; Irvine and Fukuwaka, 2011). While overfishing and spawning habitat degradation influence overall population dynamics (Nehlsen *et al.*, 1991; Slaney *et al.*, 1996; Bradford and Irvine, 2000), records show that Pacific salmon abundance closely tracks low-frequency climate shifts associated with the position and strength of the Aleutian Low pressure centre, and sea surface temperatures (SSTs) (Beamish and Boullion, 1993; Beamish *et al.*, 1997; Mantua *et al.*, 1997; Finney *et al.,* 2000). Unfortunately, the short duration of both climate and salmon abundance records in the North Pacific limits understanding of the interaction between the two systems to the past century.

Proxy records developed from sediment and tree-ring data provide an opportunity to extend these limited records. For example, Finney (1998), Finney *et al.* (2000) and Gregory-Eaves *et al.* (2009) used $\delta^{15}N$ records from lake sediment to reconstruct salmon abundance in Alaska over the past 300 years. Drake *et al.* (2002) and Drake and Naiman (2007) also established relationships between migrating salmon and nutrient-limited riparian tree-ring growth to reconstruct salmon abundance records extending from 300-150 years in Alaska, British Columbia and Oregon. Drake *et al.* (2009) describes how, in combining these above two approaches, researchers have provided insights into salmon population changes over millennial timescales. While these reconstructions provide some insight into long-term salmon population dynamics, the required site conditions necessary for using these approaches has typically limited research to small-scale investigations of individual populations migrating to specific lakes or small streams. Consequently, the long-term trends of many individual and regional Pacific salmon populations remain poorly understood.

The research presented in this paper uses annually-resolved tree-ring records to offer long-term insights about climate-induced trends in Pacific salmon populations. While previous researchers have used riparian tree ring-width growth patterns to reconstruct abundance of individual salmon populations, the significant relationships between salmon survival and large-scale ocean and atmospheric conditions presents an alternative means for reconstructing population trends at a larger regional scale. This research capitalizes on the influence of large-scale ocean and atmospheric forcings on both

tree-ring growth and west central British Columbia salmon stocks to generate a long-term history of regional salmon abundance.

3.2 Research Background

Pacific salmon are anadromous in nature. Sockeye (*O. nerka*) may spend up to the first three years of their life in nursery lakes before migrating to the ocean, while other species of salmon including chum (*O. keta*) and pink (*O. gorbuscha*) may reside in freshwater for only a few weeks prior to entering the ocean (Pearcy, 1992). Upon entering ocean waters, salmon migrate hundreds of kilometres from their natal habitats to feed on plankton and other fish (Pearcy, 1992). Chum, sockeye, coho (*O. kisutch*) and chinook (*O. tshawytscha*) salmon may spend between 2-6 years in the ocean, while the marine residence time of pink salmon is typically only 18 months (Pearcy, 1992). Nearing the end of their lives Pacific salmon return to their natal freshwater habitat to spawn and die.

Ocean and atmospheric conditions affect the ability of salmon to grow and survive during the period spent in the ocean (Downton and Miller, 1998). Large-scale ocean and atmospheric oscillations affecting the North Pacific are largely regulated by the strength and position of the Aleutian Low pressure centre (Overland *et al.*, 1999). During periods characterized by a strong Aleutian Low, winter storm tracks typically shift northward and bring increased winter precipitation and runoff to northern British Columbia and Alaska. This shift triggers well-documented changes in SSTs, ocean water-column stability, nutrient abundance, and zooplankton and phytoplankton production (Beamish and Bouillon, 1993; Gargett, 1997; Mantua et al., 1997; Stahl et al., 2006).

Brodeur and Ware (1992), Hare and Francis (1995) and Sugimoto and Tadokora (1997) show that salmon stocks in the Northeast Pacific Ocean respond quickly to this northward shift and demonstrate marked increases in productivity. The advantageous conditions associated with a stronger Aleutian Low are limited to the ocean off Alaska and northern British Columbia; regions further south along the southern British Columbia and western United States coastlines experience a concurrent decrease in the upwelling of cool nutrient-rich waters leading to declines in the resident salmon populations (Gargett, 1997).

3.3 Study Area

This study focuses on anadromous salmon populations returning to rivers and lakes along the central British Columbia coastline approximately between 51°30'-54°30' N. (Figure 3.1). Northern populations of salmon returning to spawn in this region chiefly migrate through Chatham Sound and up the Skeena River at Telegraph Passage (Gottesfeld and Rabnett, 2008). The Skeena River flows westward through the Coast Mountains and drains 54,400 km^2 of interior mountain ranges and high-elevation plateaus located within west central British Columbia. Large tributaries of the Skeena, including the Babine and Bulkley rivers, provide essential spawning and nursery habitat for five species of Pacific salmon (Gottesfeld and Rabnett, 2008).

South of Telegraph Passage and the Skeena River, salmon return to streams draining either small coastal islands or small areas of the coastal mainland. Further to the south, salmon migrate up the Burke and Dean channels to enter westward draining watersheds originating on the Chilcotin Plateau.

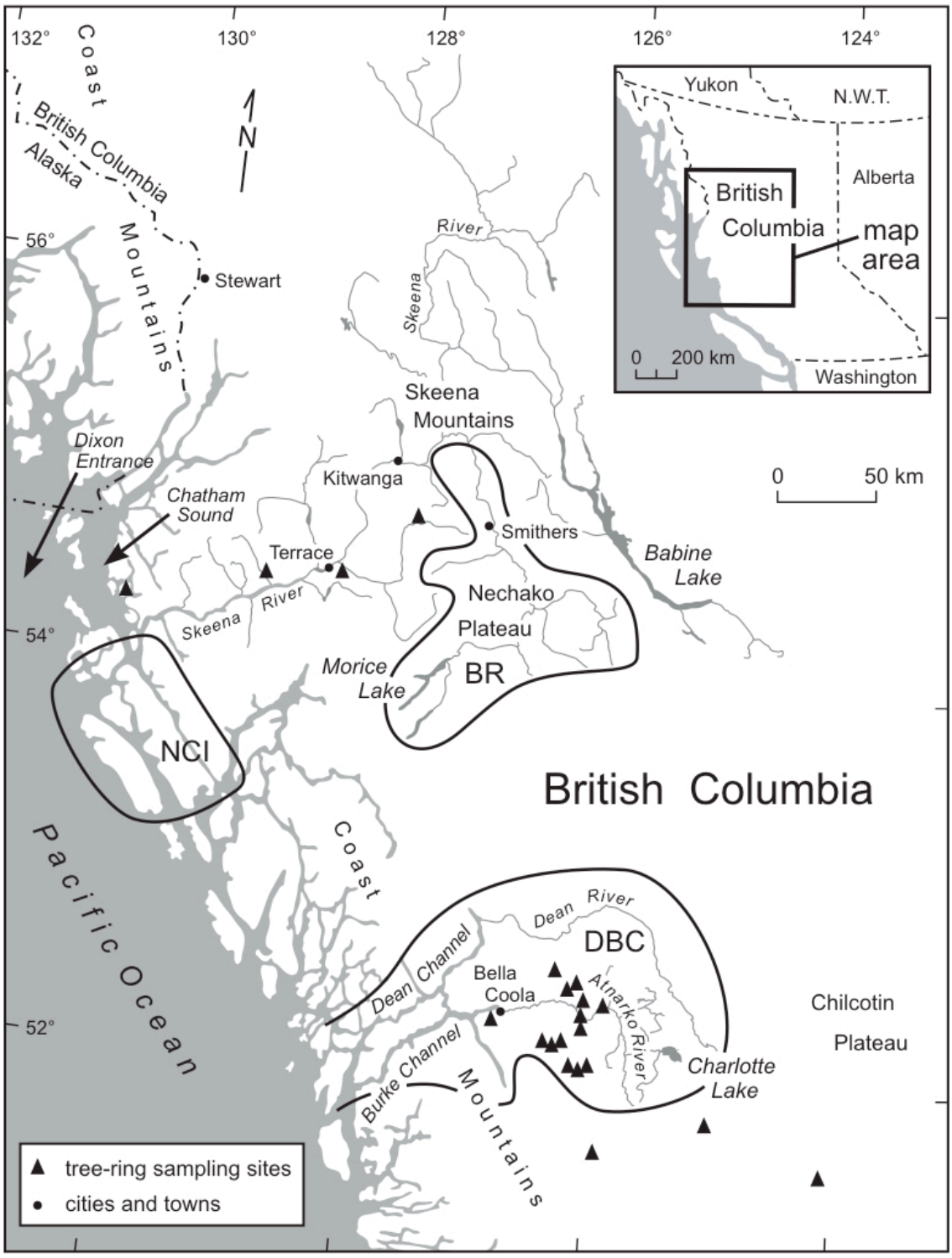

Figure 3.1 Map of the west central British Columbia coastline. The three areas outlined in black represent the approximate terrestrial boundaries for the three regional populations of Pacific salmon examined in this study, the Bulkley River (BR), North Coastal Islands (NCI), and the Dean and Burke Channels (DBC).

Headwaters regions of many of the larger salmon-bearing rivers examined fall within the Engelmann Spruce–Subalpine Fir biogeoclimatic zone and are characterized by mixed and homogeneous stands of Douglas-fir (*Pseudotsuga menziesii*), Engelmann spruce (*Picea engelmanni*), subalpine fir (*Abies lasiocarpa*), whitebark pine (*Pinus albicaulis*), logdepole pine (*Pinus contorta*) and amabilis fir (*Abies amabilis*) (Meidinger and Pojar, 1991). Downstream and coastal regions are located within the Western and Mountain Hemlock biogeoclimatic zones and are distinguished by stands of mountain hemlock (*Tsuga mertensiana*), western hemlock (*Tsuga heterophylla*), Douglas-fir, subalpine fir, yellow cedar (*Callitropsis nootkatensis*) and western redcedar (*Thuja plicata*) (Meidinger and Pojar, 1991).

Climates along the British Columbia coastline are maritime in nature with moderate temperatures and large amounts of precipitation (Moore *et al.*, 2010). Further east, high-elevation plateaus are located in the rainshadow of the Coast Mountains and are characterized by a cooler, drier, continental climate. Seasonal climate variability in this region is largely attributable to shifts in large-scale ocean and atmospheric climate patterns (Moore and McKendry, 1996; Shabbar *et al.*, 1997; Stahl *et al.*, 2006; Whitfield *et al.*, 2010). Observed fluctuations in these large-scale forcing mechanisms influence climate and ocean conditions at interannual (e.g. El Niño-Southern Oscillation, ENSO) and interdecadal (e.g. the Pacific Decadal Oscillation, PDO, the Arctic Oscillation, AO, and the Pacific North American pattern, PNA) scales (Philander, 1990; Trenburth and Hurrell, 1994; Mantua *et al.*, 1997; Overland *et al.*, 1999).

3.4 Data and Methods

A dendroecological modelling approach was used to develop long-term proxy records of climate-driven salmon abundance from escapement records (estimates of salmon returning to spawn) in west central British Columbia. A regional network of climate-sensitive tree-ring measurements was collected within the study area to provide a proxy for pre-instrumental large-scale climate variability. Correlation analysis was used to establish the nature and magnitude of relationships between salmon escapement trends, large-scale ocean and atmospheric climate forcings, and tree-ring growth patterns. Select tree-ring chronologies that correlated significantly with salmon escapement estimates were used in multivariate linear regression models to construct proxy records of climate-induced variations in salmon abundance. Persistent periods of above and below average salmon return were identified and related to temporal fluctuations in atmospheric teleconnection indices (ATIs).

3.4.1 Tree-Rings and Large-Scale Climate

Dendroclimatic research in Pacific North America has established that radial tree growth in this region records changes in climate that accompany shifts in large-scale ocean and atmospheric forcings (Gedalof and Smith, 2001a; D'Arrigo *et al.*, 2003). In west central British Columbia, warm phase PDOs, stronger Aleutian Low pressure centres and El Niño events tend to produce warmer winter, spring and summer conditions (Stahl *et al.*, 2006). Such warm climatic conditions promote earlier bud and needle maturation and lengthen the period of active photosynthesis, thereby enhancing annual ring growth (Peterson

et al., 1990; Peterson and Peterson, 2001; Peterson *et al.*, 2002; Grossnickle and Russell, 2006). By contrast, cool phase PDOs, weakened Aleutian Low pressure centres and La Niña events are associated with cool winters distinguished by large seasonal snowpacks (Stahl *et al.*, 2006). These contrasting sets of conditions act to delay bud development and photosynthesis, and lead to reduced ring growth (Gedalof and Smith, 2001b; Peterson and Peterson, 2001; Peterson *et al.*, 2002).

Tree-ring samples were collected as increment cores from mature living and standing dead trees located throughout west central British Columbia from 1997-2010. Ring-width measurements were obtained by extracting two 5-mm cores positioned 90°-180° from each other near the tree base. A third 12-mm core was collected from selected trees to provide wood density measurements.

Cores were transported to the University of Victoria Tree-Ring Laboratory where they were processed using standard dendrochronological techniques (Stokes and Smiley, 1964). Five-mm cores were air-dried, mounted to slotted boards and progressively sanded to a 600-grit polish. Ring-widths were measured to 0.01 mm from high-resolution scanned images using WinDendro (Version 2008g) software (Guay *et al.*, 1992).

Twelve-mm cores were mounted flush to wooden blocks allowing for a 2-mm thick lath to be cut from each using a Waltech high-precision twin-bladed saw (Haygreen and Bowyer, 1996). Water and resin were removed from the laths using an acetone Soxhlet apparatus (Schweingruber *et al.*, 1978; Jensen, 2007). Laths were then scanned along 50-μm intervals for 20 μs using a digital ITRAX densitometer fitted with a Chromium tube. Ring-width and maximum wood

density values were measured from the digital x-ray images using WinDendro (Version 2008g) software.

Narrow marker rings were identified and used to visually cross-date each ring-width series into site-specific chronologies (Stokes and Smiley, 1964). Independent verification of the cross-dated chronologies was completed using COFECHA (Holmes *et al.*, 1986). Cross-dating correlations were calculated over 50-year intervals with a 25-year lag and were considered statistically significant at the 0.01 level (Grissino-Mayer, 2001). The maximum wood-density chronology was similarly cross-dated and verified using the accompanying ring-width measurements. Individual series not significantly correlated to the master chronology were removed to ensure capture of a common signal. Where tree ages indicate the presence of multiple age cohorts, the series from younger trees were selectively removed to create long-lived master chronologies. Cross-dated site-specific chronologies were combined into regional species-specific master chronologies.

Master chronologies were conservatively detrended and standardized using ARSTAN (Holmes *et al.*, 1986). Age-growth related trends were first removed from individual series by fitting either a negative exponential curve or a linear regression line through the mean (Fritts, 1976). Following this, non-climatic signals within the series were removed using a cubic smoothing spline with a 67% frequency-response cutoff to ensure that 50% of the variance in ring-growth was maintained at a frequency of two-thirds the length of the series (Cook and Krusic, 2005). Standardized chronologies were built using a robust biweighted mean, providing a measure of the common signal between all series.

Residual chronologies were also constructed by removing the low-order autocorrelation from standardized chronologies, thus limiting the influence that growth from the prior year has on growth in the current year (Cook and Krusic, 2005). Expressed population signal (EPS) values were calculated for each chronology to identify where decreasing sample depth had a significant influence on ring-width variation (Wigley *et al.*, 1984; Cook and Krusic, 2005).

3.4.2 Pacific Salmon and ATI Data

Annual escapement estimates, specific to salmon species and region, were obtained from the Canadian Department of Fisheries and Oceans (Spilsted and Spencer, 2009). Composite escapement records for three sub-regions of the west central British Columbia coastline were selected as representatives of the different escapement habitats (Table 3.1). As a major tributary of the Skeena River, combined escapement records for the Bulkley River (BR) region including populations spawning in Morice River and Lake, were selected to represent populations of salmon returning to the north-central mainland of British Columbia (Figure 3.1). Likewise, composite escapement records for salmon returning to areas surrounding the Grenville Channel and to streams on Pitt, Banks, McCauley and Porcher islands represent north-central coastal island (NCI) salmon populations while records of salmon migrating up the Dean and Burke channels (DBC) represent populations returning to the south-central mainland. Although some escapement estimates are available prior to 1950, only records from 1950-2009 provide continuous records for all species of salmon in the three sub-regions examined.

Table 3.1 Salmon escapement regions

Region Title	ID	DFO Area[1]	Region Description	Record Length
Bulkley River	BR	4	Bulkley and Morice rivers	1950-2009
North Coast islands	NCI	5	Pitt, Banks, McCauley and Porcher islands Grenville channel	1950-2009
Dean/Burke channels	DBC	8	Dean and Burke channels Dean and Bella Coola rivers	1950-2009

[1]Canadian Department of Fisheries and Oceans defined regions of the British Columbia coastline

Monthly mean records for the PDO, the PNA and the AO were retrieved from the Joint Institute for the Study of the Atmosphere and Ocean website (JISAO, 2011). Monthly records for the Southern Oscillation Index (SOI) and the NINO 3.4 index both describing variability in the ENSO, were respectively obtained from the Australian Bureau of Meteorology (ABM, 2011) and the National Center for Atmospheric Research (NCAR, 2010) websites. Monthly mean records were averaged into annual and seasonal means. In accordance with previous research (e.g. Mantua *et al.*, 1997; Overland *et al.*, 1999), the winter season was defined as the mean index value for the December-February (d) period. Periods for the spring (March-May, m), summer (July-August, j) and autumn (September-November, s) seasons were similarly defined.

3.4.3 Relationships between Tree-Rings, ATIs and Pacific Salmon

Correlation analyses were used to assess the strength and significance of relationships between tree-ring growth, ATIs and salmon escapement estimates. Initially, correlation analyses between master tree-ring chronologies and, annual and seasonal mean ATI records were completed to confirm the presence of a significant regional climate signal in the tree-growth measurements.

Dendroclimatic research in Pacific North America has established that the climate signals recorded in tree-ring measurements differ with tree species and sampling environments (Laroque and Smith, 2003; Larocque and Smith, 2005a). Cores were thus collected from a variety of species growing at both high- and low-elevation locations to provide a robust regional representation of tree growth within the study area. Master chronologies demonstrating statistically significant correlations to at least one of the five ATIs were deemed sufficiently sensitive to large-scale climate forcings and were therefore used in further analyses. For these and all subsequent correlation analyses, results were considered statistically significant at the 0.05 level.

Correlation analysis was also used to establish the presence of significant relationships between salmon escapement records and large-scale ocean and atmospheric circulation patterns. Previous research on Pacific salmon life histories indicates that salmon survival is influenced by prevailing synoptic pressure systems and SSTs in both the year a salmon returns to freshwater and the prior years spent living in the ocean (Downton and Miller, 1998). Recognizing the interannual influence of large-scale forcings on salmon survival, correlations were calculated between salmon escapement records and the current (Lag-0) and prior four years (Lag-1 to Lag-4) of annual and seasonal ATIs.

Finally, correlations were calculated between selected salmon escapement records and master tree-ring chronologies. It was postulated that tree-ring chronologies significantly correlated to ATIs would provide a useful proxy for the fluctuations in the large-scale ocean and atmospheric forcings shown to influence

salmon populations. As such, current (Lag-0) and lagged (Lag-1 to Lag-4) tree growth records were considered in the correlation analyses.

3.4.4 Reconstructions of Pacific Salmon Abundance

Linear regression models were constructed for salmon escapement records significantly correlated to both ATIs and tree-ring growth records. Master chronologies significantly correlated to salmon escapement records were considered as predictor variables in each regression model. All possible combinations of predictor variables were constructed into a suite of candidate models and evaluated using correlation coefficient (R) statistics. The candidate demonstrating the strongest composite R statistic was identified and further tested to assess the predictive capabilities of the model prior to reconstructing trends in salmon abundance.

Reconstruction models were independently verified using a leave-one-out process designed to allow for model calibration over the entire period of record (Gordon, 1982). For each reconstruction, individual linear regression models were produced for each year of escapement record. A different datum year was removed from each regression model prior to calibration and was subsequently used to predict the missing escapement value. The predicted values were combined and compared to actual escapement data using verification R (Rv) statistics. Additional evaluations of model quality were completed using coefficient of variation (R^2) and reduction of error (RE) statistics (Fritts, 1976). All models displaying significant Rv statistics between leave-one-out predicted

records and escapement records, strong R^2 statistics and positive RE statistics were considered sufficient for reconstruction.

Anomalies in the proxy records were calculated as standard deviations from the long-term mean for escapement records, allowing for comparisons between the different reconstructions of salmon return. Intervals of persistently above and below average salmon return were identified. Wavelet analysis using a Gaussian 2 function and a 5% red-noise reduction was used to identify the frequency of any cyclical patterns present in the reconstructed salmon records (Torrence and Compo, 1998; http://paos.colorado.edu/research/wavelets).

3.5 Results

3.5.1 Tree-Ring Chronologies

In total, 21 tree-ring chronologies from five tree species including Douglas-fir (DF), subalpine fir (SF), mountain hemlock (MH), whitebark pine (WBP) and yellow cedar (YC) were collected (Table 3.2). As tree ages in the YC and DF chronologies indicated the presence of two distinct age cohorts, all YC series <500 years and all DF series <300 years in age were removed. Regional ring-width master chronologies were compiled from SF, DF, MH and WBP site chronologies (Table 3.3). The YC ring-width chronology and the SF maximum ring-density (SFd) chronology were considered single-site master chronologies.

Table 3.2 Tree-ring chronology sampling locations

Sampling Site	Species	Data	Sampled	Latitude/Longitude	Elevation (m asl)
Cable Spur	mh	w	2005	54°50' N, 127°48' W	1090
Copper Mountain	mh	w	2005	54°30' N, 128°28' W	887
Clayton Falls	yc	w	2010	52°17' N, 126°53' W	874
Exstew River	mh	w	2005	54°29' N, 129°07' W	875
Fisheries Pool	df	w	2010	52°23' N, 126°05' W	192
Hammer Lake	sf	w	2010	52°12' N, 126°19' W	1291
Jacobson G.	sf	w	2010	52°04' N, 126°08' W	1477
	sf	d	2010	52°04' N, 126°08' W	1477
	wbp	w	2010	52°04' N, 126°09' W	1469
Liberty Glacier	wbp	w	2001	51°35' N, 124°05' W	1525
Mount Hayes	mh	w	2005	54°17' N, 130°19' W	665
Noosgultch Creek	df	w	1997	52°27' N, 126°06' W	250
Nordshow Creek	df	w	1997	52°18' N, 126°06' W	650
Nusatsum Pass	mh	w	2010	52°13' N, 126°20' W	1079
	mh	w	1997	52°14' N, 126°19' W	1035
Perkin's Peak	wbp	w	2010	51°50' N, 125°03' W	1960
Siva G.	wbp	w	2001	51°39' N, 125°55' W	1500
Tweedsmuir	df	w	1997	52°24' N, 125°55' W	300
Tzeetsaytsul G.	sf	w	1997	52°35' N, 126°22' W	1260
Valley View High	df	w	1997	52°28' N, 126°13' W	1270
Valley View Low	df	w	1997	52°26' N, 126°12' W	650

G – glacier, w – width, d – density

Table 3.3 Summary statistics for master tree-ring chronologies

	Data	Range (yrs AD)	# cores	# years	Interseries Correlation	Mean Sensitivity	EPS[1] 0.85
YC	w	1035-2009	27	975	0.586	0.237	1340
SF*	w	1533-2009	143	477	0.518	0.194	1660
SFd	d	1636-2009	27	374	0.475	0.059	1790
WBP*	w	1139-2009	186	871	0.450	0.202	1400
MH*	w	1556-2009	210	454	0.524	0.234	1581
DF*	w	1400-2009	56	610	0.471	0.192	1560

[1]Date that the EPS for one predictor chronology drops below 0.85 due to decreased sample depth

Chronologies denoted with a * are species-specific regional chronologies built from more than one site-specific master chronology

3.5.2 Relationships Between Tree-Rings, ATIs and Pacific Salmon

Significant correlations were detected between all master tree-ring chronologies and at least one of the five ATIs (Table 3.4). Results indicated that tree-ring growth in this area was typically more strongly correlated with patterns

described by the PDO, PNA and AO, than those associated with variations in the ENSO (i.e. SOI and NINO 3.4). As all chronologies significantly correlated with at least one of the five ATIs, they were all considered to be useful proxies of variations in past large-scale climate conditions.

Table 3.4 Statistically significant correlations between master tree-ring chronologies and ATIs

		DF	MH	SF	SFd	WBP	YC
PDO	A		**0.26**			**0.19**	
	DJF		**0.30**	**0.32**			0.23
	MAM	0.21	**0.30**		0.24	0.22	
	JJA		**0.22**			0.24	
	SON						
PNA	A	0.36					
	DJF	0.33	**0.28**	0.35			0.36
	MAM						
	JJA			0.30	0.34	**0.23**	
	SON			-0.28			
AO	A	**-0.20**					**-0.25**
	DJF				-0.20		
	MAM						
	JJA		**-0.20**				
	SON	-0.20					
SOI	A		-0.28				
	DJF		**-0.27**				-0.30
	MAM		-0.29				
	JJA						
	SON		-0.24	-0.18	-0.20		
NINO 3.4	A		0.36	0.20	-0.19		
	DJF		**0.31**				0.35
	MAM		**0.34**	0.21			0.29
	JJA		0.33	0.19	0.22		
	SON		0.26		0.20		

A - annual mean, DJF – December-February, MAM – March-May, JJA – June-August, SON – September-November
Only correlation results statistically significant at the 0.05 level shown
Bold correlations are to standardized chronologies although significant correlations were often detected to both standardized and residual data

Salmon escapement records were significantly correlated with current and lagged terms for both master tree-ring chronologies and ATIs (Table 3.5, Figure 3.2). Six species-specific regional salmon populations were identified for

dendroecological reconstruction. The salmon escapement records not selected for reconstruction typically demonstrated fewer significant correlations to either the ATIs or the tree-ring chronologies (results not shown). Salmon escapement correlations were typically stronger and more numerous with the PDO, PNA and AO ATIs and with the YC, WBP and SFd chronologies.

Table 3.5 Correlation table for salmon escapement records and ATIs

		BR Sockeye	BR Chinook	NCI Pink	DBC Sockeye	DBC Chum	DBC Chinook
PDO	Current				-0.38 (d)	0.21 (d)	
	Lag-1			-0.23 (j)	-0.36 (a)		
	Lag-2				-0.34 (a)		
	Lag-3		0.37 (j)		-0.30 (m)		
	Lag-4		0.42 (j)				
PNA	Current				-0.31 (d)	0.28 (d)	
	Lag-1					-0.27 (d)	
	Lag-2				-0.40 (d)		-0.24 (d)
	Lag-3		0.29 (m)				
	Lag-4	0.32 (m)	0.38 (a)				
AO	Current						
	Lag-1	0.29 (d)	0.28 (d)				
	Lag-2	0.47 (d)	0.40 (j)				0.25 (a)
	Lag-3	0.34 (a)					0.31 (a)
	Lag-4					0.24 (m)	0.31 (a)
SOI	Current				0.24 (j)		
	Lag-1			0.24 (d)			-0.26 (m)
	Lag-2	-0.29 (j)					
	Lag-3						
	Lag-4	-0.29 (m)	-0.32 (m)				
NINO 3.4	Current			-0.29 (m)			
	Lag-1						
	Lag-2						
	Lag-3						
	Lag-4						

Only correlation results statistically significant at the 0.05 level shown
Where significant correlations were found between more than one of the mean values (a – annual, d – December-February, m – March-May, j – July-August, and s – September-November) only the strongest correlation result was reported.

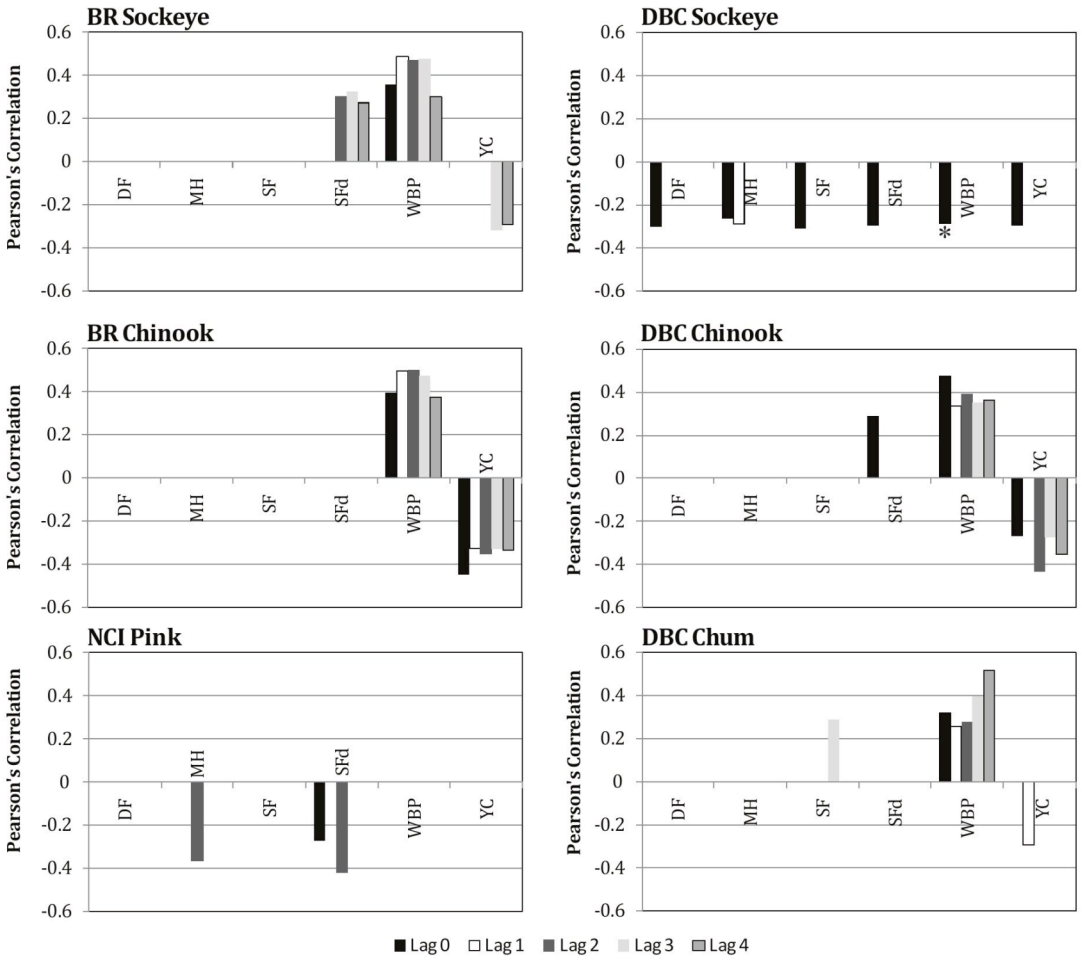

Figure 3.2 Significant correlations for the six regional populations of Pacific salmon reconstructed and master tree-ring chronologies. Where both standardized and residual master chronologies significantly correlate to Pacific salmon records only the strongest relationship is reported. The correlation denoted by a * represents a result where the strongest correlation was calculated using the residual master chronology

3.5.3 Reconstructions of Pacific Salmon Abundance

The significant relationships detected between ATIs, tree-ring growth and salmon escapement advocate the use of climate-sensitive tree-ring measurements to extend records of salmon abundance. Models were constructed and validated for the six populations of salmon noted in Figure 3.2 and demonstrated good predictive capabilities (Table 3.6). The models explained between 27-39% of the variability in escapement records and were more proficient at capturing trends

than annual magnitudes (Figure 3.3). The closely matching shifts in actual and reconstructed BR chinook salmon abundance in the 1970s well illustrates this observation. As the models cannot separate out the population dynamics induced by overfishing and habitat degradation, it is likely that changes stemming from these sources comprise the majority of unexplained variability.

Table 3.6 Summary statistics for salmon reconstructions

	R	Rv	R^2	RE	Chronologies	Proxy Record	EPS[1]
BR Sockeye	0.53	0.44	0.28	0.28	YC, WBP(L1), SFd(L2)	1638-2009	1790
BR Chinook	0.59	0.48	0.34	0.34	YC, WBP, WBP(L2)	1141-2009	1440
NCI Pink	0.52	0.43	0.27	0.27	SFd, MH(L1), SFd(L2)	1638-2009	1790
DBC Sockeye	0.55	0.44	0.31	0.34	YC, WBP*, DF, SFd*, MH(L1)	1638-2009	1790
DBC Chum	0.56	0.48	0.32	0.32	SF(L3), WBP(L4)	1533-2009	1660
DBC Chinook	0.62	0.56	0.39	0.39	WBP, SFd, YC(L2)	1638-2009	1790

* – residual chronology, L1- lag 1 year, L2 – lag 2 years, L3 – lag 3 years, L4 – lag 4 years
[1]Date that the EPS for one chronology drops below 0.85 due to decreased sample depth

As all models demonstrated good predictive capabilities, the six models were subsequently used to extend population records. Trends in the BR chinook population were extended back to 1400 AD and the model maintained sufficient sample depth over the entire period of reconstruction. Proxy records for the DBC chinook populations were extended back to 1638 AD. Although decreased sample depth in the SFd chronology is identified by a drop in EPS prior to 1790 AD, a comparison of the two chinook reconstructions indicated that the loss of sample depth did not impair the quality of the prediction. As such, all other models using the SFd chronology as one of the predictor terms (NCI pink, BR sockeye, DBC sockeye) were also confidently reconstructed back to 1638 AD. The model reconstructing trends in the DBC chum populations was reconstructed back to 1536 AD and was influenced by decreased SF sample depth prior to 1660 AD.

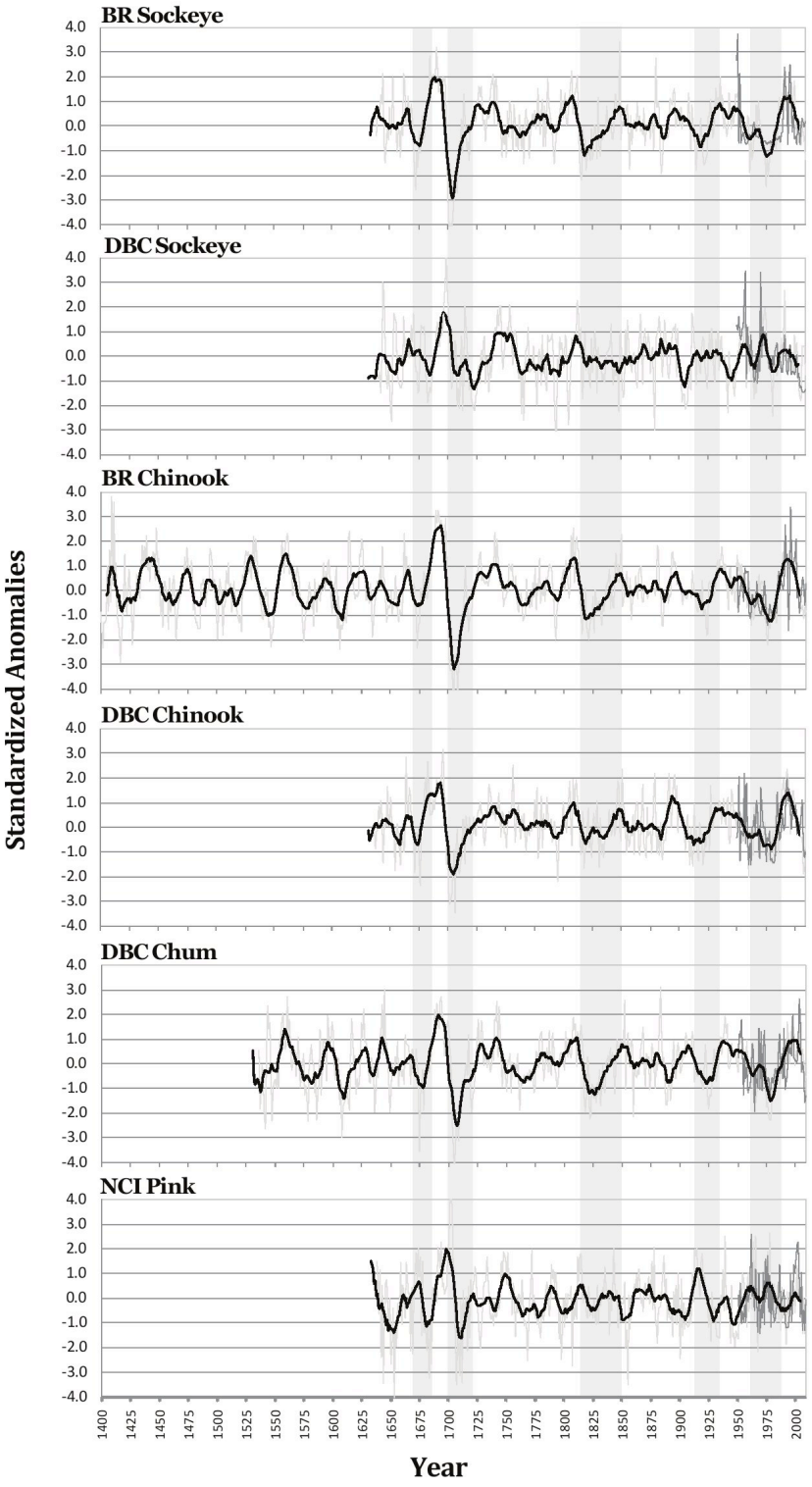

Figure 3.3 Reconstructions of salmon abundance anomalies. Gray lines are the actual reconstructions. Black lines represent a 10-year running mean of the data. Shaded gray areas illustrate intervals of synchroneity among salmon records.

Wavelet analysis of the six reconstruction models revealed common patterns of high- and low-frequency variability (Figure 3.4). A high-frequency interannual (approximately 8-15 year) wavelet function influenced all six salmon populations, likely reflecting changes in SSTs and atmospheric pressures induced by the ENSO. A second, more distinctive mode of variability described a lower-frequency interdecadal oscillation with an interval of approximately 20-50 years. This mode of variability likely reflects the influence of SSTs and the Aleutian Low pressure system on salmon survival as described by the PDO and PNA. The strength of this low-frequency signal varied over the record and was typically stronger during the late-1600s, the early- and mid-1700s, the early-1800s and the mid- and late-1900s. Prior to the mid-1600s, the BR chinook model described intervals strongly influenced by this low-frequency mode of variability during the mid- 1400s, the 1500s, and the early- 1600s. The signal waned in strength during the late-1400s (only observed in the BR chinook reconstruction), the mid-1600s, the late-1700s, the mid- and late-1800s and the early-1900s. Similar wavelet results, indicating a waning of low-frequency oscillations during the late-1800s, have previously been reported in PDO and hydroclimate conditions reconstructions from western North America (Gedalof and Smith, 2001a; Lamoureaux *et al.*, 2006; Hart *et al.*, 2010).

Reconstructions of salmon abundance used both current and lagged tree-ring growth records demonstrating and confirming the interannual influence of large-scale climate on salmon survival. The DBC chum reconstruction was the only exception, as the model for this population used only lagged WBP and YC chronologies. Evidence indicates that chum salmon, entering the ocean after only

several weeks in the freshwater environment, are most affected by SSTs and plankton abundance during the earlier stages of life (Downton and Miller, 1998). It was therefore expected that chum populations would demonstrate stronger correlations with lagged tree-ring and ATI records.

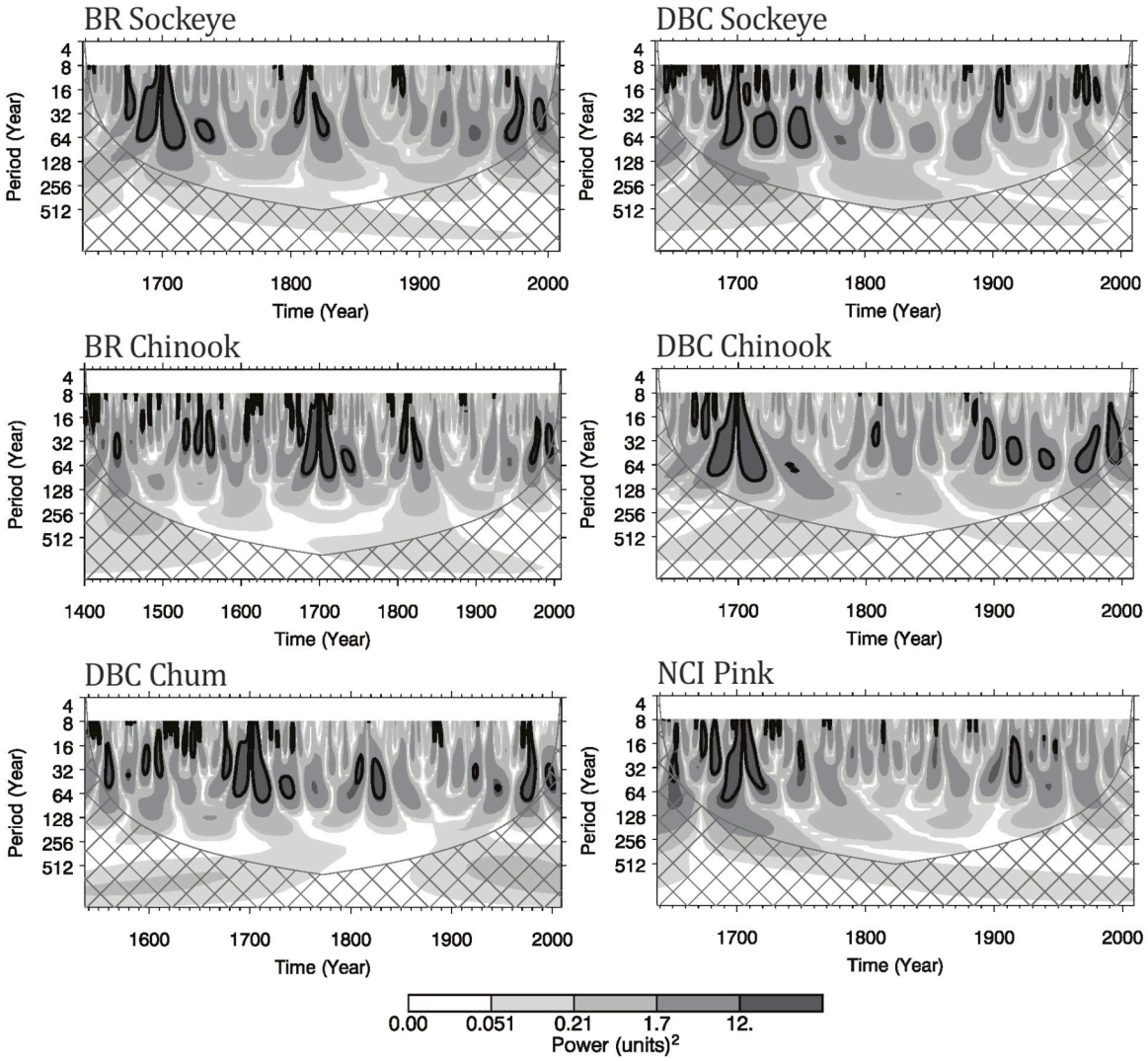

Figure 3.4 Wavelet power spectrums for the six salmon abundance reconstructions. The wavelet power spectrum uses a Gaussian-2 function. Cross-hatched regions of the wavelet diagrams represent the cone of influence where zero-padding of the data was used to reduce variance. Black contours indicate significant modes of variance with a 5% significance level using an autoregressive lag-1 red-noise background spectrum (Torrence and Compo, 1998).

3.6 Discussion

3.6.1 Reconstructions of Pacific Salmon Abundance

Models describe alternating intervals of above and below average salmon abundance throughout the past six centuries (Figure 3.3). Proxy reconstructions for the BR sockeye population, the BR chinook population and the DBC chinook population portray largely synchronous trends in salmon abundance over the common period from 1638-2009. Notable departures of below average salmon abundance for these three populations were depicted around 1670-1680, 1700-1720, 1820-1850, 1920-1930 and 1960-1980. Generally above average salmon abundance was inferred during the 1690s, the 1720s-1760s, the early-1800s, the 1890s, the early-1900s, the 1940s-1950s and the period following 1980. Although less distinct, predicted trends for the DBC chum population also tracked these oscillations in salmon abundance. The similarities between trends describing the sixty-year escapement records for these four salmon populations corroborate findings using the tree-ring reconstructions (Figure 3.5).

Prior to 1638 AD the BR chinook reconstruction, extending to 1400 AD, and the DBC chum reconstruction, extending to 1536 AD, predict further intervals of above and below average salmon abundance. Models describe thriving salmon populations around 1440-1450, the 1470s, the mid-1520s to 1550, the 1560s, the very early-1600s and the 1620s. In contrast, periods of lower than average salmon return were modelled during the 1420s-1430s, the 1450s-1470, the 1550s, the 1580s, and the 1610s.

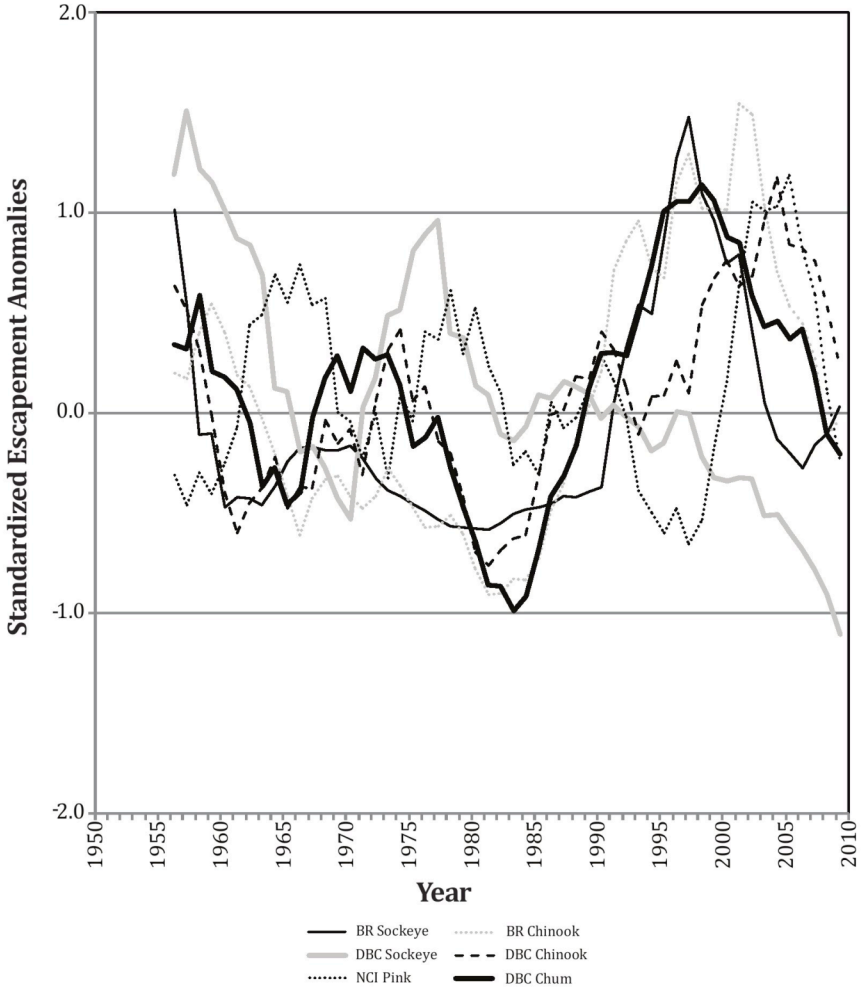

Figure 3.5 Seven-year running mean trend lines of the six escapement records modelled using climate-sensitive tree-ring measurements.

Trends describing fluctuations in sockeye salmon returning to the DBC region were not synchronous with trends in the BR sockeye, BR chinook, DBC chinook and DBC chum populations. Reconstructed evidence instead suggests that this regional population typically responded out-of-phase with other populations in the area. The distinct trends detected for the two sockeye salmon populations may mark the transition between northern and southern salmon populations that typically behave out-of-phase from each other (Mantua *et al.*, 1997).

As demonstrated by the escapement record trends in Figure 3.5, it was not expected that the pink salmon returning to the NCI region would track the trends found in other populations. Reconstructed records confirm that trends in the NCI pink salmon populations typically changed abruptly or were out-of-phase with trends in other salmon populations. As pink salmon spend only a short period of time in the ocean, this difference in the nature and timing of abundance likely reflects the different life histories of Pacific salmon.

3.6.2 Comparisons with Other Proxy Records of Salmon Abundance

The six paleorecords of salmon abundance corroborate findings from related studies. Nutrient-limited riparian tree derived proxy records of individual chinook and chum populations migrating to streams in Oregon and Alaska, indicate declines in escapement that coincide with lower than average abundance predicted during the early-1700s, mid-1800s and mid- to late-1900s (Drake and Naiman, 2007). Independent verification of these negative departures was achieved by comparing the six proxy records with constructions of salmon abundance inferred using fluctuations in the nutrient concentrations of lake sediments from Alaska (Finney, 1998; Finney *et al.*, 2000). A recent study investigating the relationship between lake sediment and salmon abundance indicates that salmon migrating to small Alaskan lakes also experienced earlier declines in population levels during the past two millennia (Drake *et al.*, 2009). These inferences, however, are made at a much lower temporal resolution than the insights gained by this research.

3.6.3 Climate Connections

The distinct low- and high-frequency modes of variability identified in the six reconstructions suggest the relationship between salmon and large-scale climate forcings has persisted throughout the past six centuries. The low-frequency mode of variability in salmon stocks likely reflects shifts in the Aleutian Low pressure centre and the accompanying changes in SSTs and related plankton abundance. The alternating intervals describing a waning and strengthening of this signal may illustrate periods where salmon populations are less responsive to these changes in large-scale climate or intervals of time where large-scale climate conditions were less variable. Regardless of the cause, information about the presence and strength of these low-frequency climate-driven fluctuations is likely to be valuable to fisheries managers when planning strategies for managing salmon stocks.

3.7 Conclusion

This research demonstrates the value and potential of reconstructing trends in regional Pacific salmon populations using climate-sensitive tree-ring chronologies. It represents the first study to successfully reconstruct annual-resolution records of regional salmon abundance for populations returning to western North America, and is the first to use both ring-width and ring-density parameters in a salmon abundance model. The advances made in this study soundly establish a novel method for investigating the long-term variability of Pacific salmon at a wider regional scale than previous techniques have allowed.

Given that the proxy records are able to characterize climate-driven fluctuations in regional salmon populations, their trends also indicate a long-term influence of large-scale climate on Pacific salmon. The strong similarities between these and previously published proxy records of salmon abundance suggest that long-term fluctuations in salmon population levels are primarily climate related. In addition to offering new evidence to suggest that Pacific salmon are a naturally dynamic population that collapsed during the early-1700s, mid-1800s and late-1900s, this paper has indirectly identified previously unknown declines in British Columbia salmon abundance during the 1400s, 1500s and early-1600s. The tendency for Pacific salmon populations to naturally collapse and flourish, as demonstrated in the proxy records spanning the past six centuries, should be a source of valuable information for those trying to manage and regulate this ecologically, culturally and economically important resource.

Chapter 4

Summary and Conclusion

Based on tree-ring records, this research provides new long-term information about climatic conditions, nival-river runoff, and Pacific salmon abundance in west central British Columbia. A multi-species regional network of tree-ring measurements was assembled using new and archived chronologies collected in the study area, allowing for reconstructions of the aforementioned variables across a spatially extensive range. This study also assessed and confirmed the long-term influence of large-scale ocean and atmospheric oscillations on the natural dynamics of these environmental variables. This concluding chapter offers a summary of the research, discusses connections between the core research contributions described in Chapters 2 and 3, addresses the limitations of this study, and outlines opportunities for further research.

4.1 Summary of Findings

4.1.1 Hydroclimate Reconstructions

Late melt-season (July-August) mean runoff was reconstructed for the Atnarko and Skeena rivers back to 1660 AD. These records represent the first

dendrohydrologic reconstructions of nival rivers in British Columbia and thus provide the first long-term insights into their past behavior. The records are characterized by alternating intervals of persistently above and below average discharge. Strong negative departures in runoff are apparent during the early- to mid-1700s and the early- and mid-1900s. Strong positive departures characterize the late-1600s, the very early-1700s, the early-1800s and parts of the early- and mid-1900s. Several periods of highly anomalous runoff during the 350-year history describe events more extreme than those that occurred within the instrumental record. The natural occurrence of high- and low-flow events of this magnitude may provide valuable insight for managers of British Columbia freshwater resources.

A second goal of this research was to assess the long-term influence of regional and large-scale climate conditions on nival-river discharge. As such, tree-ring proxy records for summer (June-August) temperature, end-of-winter (May 1) snow water equivalent (SWE) and winter (October-February) Pacific North America pressure (PNA) anomalies were constructed back to 1660 AD. A visual comparison of records illustrates that periods of higher than average melt-season runoff are synchronous with intervals of above average SWE, below average summer temperature and below average PNA. Correlation and wavelet analyses of these extended discharge records confirms the influence of large-scale ocean and atmospheric forcings including the Pacific Decadal Oscillation (PDO), the PNA and the El Niño-Southern Oscillation (ENSO) on nival-river regimes in west central British Columbia.

4.1.2 Pacific Salmon Reconstructions

Abundance records for four species of Pacific salmon (chinook, sockeye, chum and pink) were constructed using a regional network of tree-ring measurements. In contrast to previous spatially-limited reconstructions of Pacific salmon (Finney, 1998; Finney *et al.*, 2000; Drake and Naiman, 2002; Drake *et al.*, 2007), this study demonstrated the value of using climate-sensitive tree-ring growth measurements to construct a broad regional history of salmon abundance. As this study is the first to reconstruct records of Pacific salmon using this method, it represents a significant contribution to the field of paleoecological modelling.

The reconstructed salmon abundance records vary in length and extend from 1400, 1536 and 1638 AD to present. The records are characterized by oscillating intervals of higher and lower than average salmon return. Chinook, chum and north central sockeye populations fluctuate in synchrony, while populations of south central sockeye and pink fluctuate with differences in timing. Regardless of these differences, significant collapses of salmon stocks mark the early-1400s, the late-1500s, the late-1600s, the early-1700s, the early- and mid-1800s and parts of the 1900s. Significant intervals of increased salmon abundance distinguished the mid-1400s, the mid-1500s, the early-1600s, the mid-1700s, the early- and late-1800s and parts of the early-, mid- and late-1900s.

Correlation and wavelet analyses confirm the long-term influence of large-scale ocean and atmospheric fluctuations described by the PDO, the PNA and the Arctic Oscillation (AO) on salmon abundance. To a lesser extent, climate oscillations related to the ENSO also appear to have a significant influence on the

natural dynamics of salmon populations. These findings support evidence from previous studies, indicating that Pacific salmon abundance is strongly controlled by climate fluctuations. Considering these long-standing climate driven trends in salmon stocks may be an important strategy towards the continued management of this economically and ecologically important resource.

4.2 Runoff, Climate and Pacific Salmon Connections

This research described past trends in river runoff, climate conditions and Pacific salmon abundance. The anadromous nature of Pacific salmon exposes their populations to changes in both marine and freshwater environments. Research has demonstrated that fluctuations in river runoff can influence salmon population levels (Beamish *et al.*, 1994; Rand *et al.*, 2006; Gottesfeld and Rabnett, 2008). Years with anomalously high discharge and warm freshwater temperatures are often associated with lower than average salmon abundance in subsequent years. Above average discharge and warm stream temperatures necessitate an increase in the energy expended by salmon during their upstream migration that can lead to an increase in salmon mortality (Beamish *et al.*, 1994; Rand *et al.*, 2006). In turn, increased mortality of spawning salmon decreases the number of hatchlings in the following spring and thus the number of returning salmon in subsequent years.

Exploratory correlation analysis between Skeena River runoff records and the two Bulkley River (BR) escapement records for populations reconstructed in Chapter 3 reveal significant relationships between runoff and salmon return in the current and subsequent years (Table 4.1). Sockeye and chinook populations

both demonstrate significant correlations to Skeena River discharge records. The negative correlation identified between runoff and sockeye escapement in the current year likely reflects the difficulty of upstream migration during above average runoff conditions. The negative correlations detected between runoff and salmon return in subsequent years were likely a consequence of the reduced number of spawners and hatchlings following above average runoff conditions.

Table 4.1 Correlations between Skeena River discharge and salmon escapement

		Skeena Mean Discharge			
	Year	January-March	April-June	July-September	October-December
BR Sockeye	Current			-0.273	
	+1				
	+2		0.270	-0.311	
	+3		0.349	-0.286	
	+4				
BR Chinook	Current				
	+1				
	+2				-0.288
	+3			-0.276	-0.268
	+4				

Only correlation results statistically significant at the 0.05 level are shown

4.3 Research Limitations and Opportunities

4.3.1 Improving Models for Salmon Abundance

The six tree-ring models of salmon abundance constructed for populations in west central British Columbia significantly improve the understanding of natural fluctuations in Pacific salmon stocks. Constraints in data availability prevent the inclusion of annual salmon catch estimates to supplement escapement estimates. As such, the tree-ring models calibrated solely with escapement data were not capable of commenting on stock variability caused by

fluctuations in commercial catch abundance. It was postulated that with the inclusion of catch data, model prediction capabilities would significantly improve. An exploratory investigation testing this hypothesis was undertaken using shorter (23 year) records of Pacific salmon abundance that include estimates of catch (Appendix C). The results from this exploratory study indicate that if longer estimates of salmon catch could be obtained for west central British Columbia further insights on the long-term population dynamics of Pacific salmon might be attained.

4.3.2 Comparing Multiple Tree-Ring Proxy Records

Trend similarities identified between paleoenvironmental records constructed using related sources (e.g. two tree-ring records) must be considered with caution. In such cases it is possible that at least a portion of the observed similarity reflects the parallels between predictor variables rather than connections between predicted variables. In an effort to limit this concern, comparisons made between tree-ring proxy records were also accompanied, wherever possible, by comparisons made using independent proxy records. Sources for these independent proxy records include anomalies in annual varve thickness, periods of recognized glacial advance, variations in the nutrient concentrations of lake sediments and tree-growth from nutrient-limited climate-insensitive riparian forests. In all cases the trends described by independent proxy records closely matched findings from this study. The use of tree-ring measurements from five different species of tree growing in a diversity of environments was also considered to improve the confidence of the results. With

these considerations, the proxy records presented in this thesis were deemed adequate representations of past conditions and were thus used to compare trends in the paleoenvironmental record. As the spatial and temporal depth of proxy records derived from alternate sources improves further verification of these findings may become possible.

4.3.3 Spatial Coverage of a Regional Tree-Ring Network

The regional network of tree-ring chronologies constructed for this thesis utilized new and archived tree-ring samples. The resultant network was assumed to constitute a robust regional representation of tree growth in west central British Columbia. Within this network there was a higher concentration of tree-ring chronologies collected in the southern regions of the study area, with fewer series collected from northern regions. The addition of more tree-ring measurements in northern environments may strengthen models describing past conditions in north central British Columbia. Tree-ring growth measurements collected for temperature-sensitive Engelmann spruce may also prove beneficial for future research in this region and would provide a sixth species of tree in the multi-species tree-ring network.

4.3.4 Building a Multi-Species Ring-Density Network

The tree-ring models of river runoff, end-of-winter SWE and salmon abundance introduced in this thesis are the first in Pacific North America to include wood density measurements. Comparisons between models utilizing both ring-density and ring-width chronologies and models utilizing only ring-width

chronologies demonstrate the value of incorporating wood density variables in dendrohydroclimatic and dendroecologic models. Overall, models that included the subalpine fir maximum ring-density (SFd) chronology were stronger than models without it.

Wood density samples were also collected for yellow cedar (YC) and Douglas-fir (DF) trees in west central British Columbia. Unfortunately, complications arising from the varied angles of tree-rings captured in the samples led to a premature decrease in sample depth exceeding that of the SFd chronology (Table 4.2). The early loss of sample depth for these chronologies resulted in their exclusion from the pool of possible predictor variables when constructing proxy records of hydroclimate and salmon abundance. Regardless, it was expected that additional density core sampling of these sites would yield robust, climate-sensitive chronologies and improve future dendrochronologic modelling. Exploratory correlation analysis was completed for the YC and DF density chronologies and select hydroclimate records. Example results are provided and discussed in Appendix D. Results demonstrate the potential for improved dendrochronologic modelling and describe an opportunity for further research.

Table 4.2 Chronology statistics for yellow cedar and whitebark pine maximum ring-density chronologies

	Location	Elevation (m asl)	# cores	Range (yrs AD)	R	S	EPS 0.80
DF	52°22'34"N, 126°04'50"W	192	34	1569-2009	0.423	0.035	1870
YC	52°17'09"N, 126°52'34"W	874	33	1284-2009	0.475	0.070	1890

R – mean series intercorrelation, S – mean sensitivity

EPS 0.80 – Date that the EPS drops below 0.80 due to decreased sample depth. In both cases the EPS recovers above 0.80 at least once prior to the date given

4.3.5 Century-Scale Growth Patterns

A visual examination of the YC and regional whitebark pine (WBP) chronologies revealed a distinct multi-century fluctuation in ring-width growth. An exploratory analysis of these growth trends was completed and presented in Appendix E. The analysis was largely inconclusive and requires further research to properly assess this low-frequency cyclical growth pattern.

4.4 Conclusion

The results of this research offer insight into the past dynamics of nival-river runoff, air temperature, snow accumulation, synoptic climate and salmon abundance in west central British Columbia. In addition to improving the understanding of natural long-term variability in the paleoenvironment, the research makes several significant advances to dendrochronologic research in Pacific North America. The dendrohydroclimatic models constructed using the SFd chronology establish the benefits of using the climate signals captured in annual variations of wood density. Four of the six salmon abundance models introduced in Chapter 3 also utilize the SFd chronology, demonstrating that these benefits can be extended to dendroecological research. Finally, the six models of Pacific salmon abundance introduced in this thesis are the first to use climate-sensitive tree-ring growth measurements to produce proxy records of salmon escapement at a regional scale. Accordingly, these models provide advancements to the fields of dendrochronology and paleoecology.

References Cited

AHCCD (Adjusted Homogenized Canadian Climate Database website). 2010. http://www.cccma.ec.gc.ca/hccd, [20 December, 2010].

ABM (Australian Government Bureau of Meteorology website). 2011. *S.O.I. (Southern Oscillation Index) Archives*. http://www.bom.gov.au/climate/current/soihtm1.shtml, [4 January 2011].

Axelson JN, Sauchyn DJ, Barichivich J. 2009. New reconstructions of streamflow variability in the South Saskatchewan River Basin from a network of tree ring chronologies, Alberta, Canada. *Water Resources Research* **45**: 1-10. DOI:10.1029/2008WR007639.

Barnett TP, Adam JC, Lettenmaier DP. 2005. Potential impacts of a warming climate on water availability in snow dominated regions. *Nature* **438**: 303-309. DOI:10.1038/nature04141.

Bates BC, Kundzewicz ZW, Wu S, Palutifkof JP (eds). 2008. Climate change and water. *Technical Paper of the Intergovernmental Panel on Climate Change*, IPCC Secretariat: Geneva.

BC RFC (B.C. River Forecast Centre website). 2010. *B.C. Environment Historical Snow Survey Data*. http://bcrfc.env.gov.bc.ca, [5 December, 2010].

Beamish RJ, Bouillon DR. 1993. Pacific salmon production trends in relation to climate. *Canadian Journal of Fisheries and Aquatic Sciences* **50**: 1002-1016.

Beamish RJ, Neville CM, Thomson BL, Harrison PJ, St. John M. 1994. A relationship between Fraser River discharge and interannual production of Pacific salmon (*Oncorhynchus* spp.) and Pacific herring (*Clupea pallasi*) in the Strait of Georgia. *Canadian Journal of Fisheries and Aquatic Sciences* **51**: 2843-2855.

Beamish RJ, Noakes DJ, McFarlane GA, Klyashtorin L, Ivanov VV, Kurashov V. 1997. The regime concept and natural trends in the production of Pacific salmon. *Canadian Journal of Fisheries and Aquatic Sciences* **56**: 516-526.

Bitz CM, Battisti DS. 1999. Interannual to decadal variability in climate and the glacier mass balance in Washington, western Canada, and Alaska. *Journal of Climate* **12**: 3181-3196.

Bonsal BR, Shabbar A, Higuchi K. 2001. Impact of low frequency variability modes on Canadian winter temperature. *International Journal of Climatology* **21**: 95-108.

Bostock HS. 1948. *Physiographic of the Canadian Cordillera, with special reference to the area north of the fifty-fifth parallel*, Geological Survey of Canada, Report 247, Kings Printer and Controller of Stationary: Ottawa, ON.

Bradford MJ, Irvine JR. 2000. Land use, fishing, climate change and the decline of Thompson River, British Columbia, coho salmon. *Canadian Journal of Fisheries and Aquatic Sciences* **57**: 13-16.

Brodeur RD, Ware DM. 1992. Long-term variability in zooplankton biomass in the subarctic Pacific Ocean. *Fisheries Oceanography* **1**: 32-38.

Case RA, MacDonald GM. 2003. Tree ring reconstructions of streamflow for three Canadian Prairie rivers. *Journal of American Water Resources Association* **37**: 704-714.

Cook ER. 1985. *A time-series analysis approach to tree-ring standardization*. Unpublished Ph.D. dissertation, University of Arizona: Tucon, AZ.

Cook ER, Krusic PJ. 2005. *Program ARSTAN: A tree-ring standardization program based on detrending and autoregressive time-series modelling, with interactive graphics*. Columbia University, Lamont-Doherty Earth Observatory: Palisades, NY.

Coulthard, BL. 2009. *Dendroclimatological and dendroglaciological investigations at Confederation and Franklin glaciers, central Coast Mountains, British Columbia, Canada*. Unpublished M.Sc. thesis, University of Victoria: Victoria, BC.

Court A. 1962. Measures of streamflow timing. *Journal of Geophysical Research* **67**: 4335-4339.

D'Arrigo RD, Jacoby GC, Free RM. 1992. Tree-ring width and maximum latewood density at the North American treeline: parameters of climate change. *Canadian Journal of Forest Research* **22**: 1290-1296.

Davi NK, D'Arrigo RD, Jacoby JG, Buckley B, Kobayashi O. 2002. Warm-season annual to decadal temperature variability for Hokkaido, Japan, inferred from maximum latewood density (AD 1557-1990) and ring width (AD 1532-1990). *Climatic Change* **52**: 251-262.

Department of Ocean and Atmospheric Sciences. 2011. *A Practical Guide to Wavelet Analysis*. University of Colorado: Boulder, CO; http://paos.colorado.edu/research/wavelets, [20 January, 2011].

Downton MW, Miller KA. 1998. Relationship between Alaskan salmon catch and North Pacific climate on interannual and interdecadal time scales. *Canadian Journal of Fisheries and Aquatic Sciences* **55**: 2255-2265.

Drake DC, Naiman RJ, Helfield JM. 2002. Reconstructing salmon abundance in rivers: an initial dendrochronological evaluation. *Ecology* **83**: 2971-2977.

Drake DC, Naiman RJ. 2007. Reconstruction of Pacific salmon abundance from riparian tree-ring growth. *Ecological Applications* **17**: 1523-1542.

Drake, D., Finney, B., Gregory-Eaves, I. and R. Naiman. 2009. Long-term perspectives on salmon abundance: evidence from lake sediments and tree rings. In Knudsen, E., Michael, H. and Steward, C. (eds.) Pacific Salmon Environment and Life History Models: Advancing Science for Sustainable Salmon in the Future. American Fisheries Society Symposium 71: 1-11

Eaton B, Moore RD. 2010. Regional hydrology. In *Compendium of Forest Hydrology and Geomorphology in British Columbia Volume 1 of 2*, Pike RG, Redding TE, Moore RD, Winkler RD, Bladon KD (eds). British Columbia Ministry of Forests and Range, Forest Science Program: Victoria; 85-110.

Finney BP. 1998. Long-term variability of Alaskan sockeye salmon abundance determined by analysis of sediment cores. *North Pacific Anadromous Fish Commission Bulletin* **1**: 388-395.

Finney BP, Gregory-Eaves I, Sweetman J, Douglas MSV, Smol JP. 2000. Impacts of climatic change and fishing on Pacific salmon abundance over the past 300 years. *Science* **290**: 795-799.

Fritts HC. 1976. *Tree-Rings and Climate*, Academic Press: New York, NY.

Gargett AE. 1997. The optimal stability 'window': a mechanism underlying decadal fluctuations in North Pacific salmon stocks? *Fisheries Oceanographer* **6**: 109-117.

Gedalof Z, Smith, DJ. 2001a. Interdecadal climate variability and regime-scale shifts in Pacific North America. *Geophysical Research Letters* **28**: 1515-1519.

Gedalof Z, Smith DJ. 2001b. Dendroclimatic response of mountain hemlock (*Tsuga mertensiana*) in Pacific North America. *Canadian Journal of Forest Research* **31**: 322-332.

Gedalof Z, Peterson DL, Mantua NJ. 2004. Columbia River flow and drought since 1750. *Journal of the American Water Resources Association* **40**: 1579-1592.

Gordon GA. 1982. Verification of dendroclimatic reconstructions. In *Climate from Tree Rings*, Hughes MK, Kelly PM, Pilcher JR, LaMarche VC (eds). Cambridge University Press: Cambridge; 58-61.

Gottesfeld AS, Johnson Gottesfeld LM. 1990. Floodplain dynamics of a wandering river, dendrochronology of the Morice River, British Columbia, Canada. *Geomorphology* **3**: 159-179.

Gottesfeld AG, Rabnett KA. 2008. *Skeena River Fish and Their Habitat*, UBC Press: Vancouver, BC.

Gregory-Eaves I, Selbie DT, Sweetman JN, Finney BP, Smol JP. 2009. Tracking sockeye salmon population dynamics from lake sediment cores: a review and synthesis. *American Fisheries Society Symposium* **69**: 379-393.

Griesbauer HP, Green DS, O'Neill GA. 2011. Using a spatiotemporal climate model to assess population-level Douglas-fir growth sensitivity to climate change across large climatic gradients in British Columbia. *Forest Ecology and Management* **261**: 589-600.

Grissino-Mayer HD. 2001. Evaluaing cross-dating accuracy: a manual and tutorial for the computer program COFECHA. *Tree-Ring Research* **57**: 205-221.

Grossnickle SC, Russell JH. 2006. Yellow-cedar and western red cedar ecophysiological response to fall, winter and early spring temperature conditions. *Annals of Forest Science* **63**: 1-8.

Guay R, Gagnon R, Morin H. 1992. A new automatic and interactive tree-ring measurement system based on a line scan camera. *The Forestry Chronicle* **38**: 138-141.

Hamlet AF, Mote PW, Clark MP, Lettenmaier DP. 2007. Twentieth-century trends in runoff, evapotranspiration, and soil moisture in the western United States. *Journal of Climate* **20**: 1468-1486.

Hare SR, Francis RC. 1995. Climate change and salmon production in the Northeast Pacific Ocean. *Canadian Special Publication for Fisheries and Aquatic Sciences* **121**: 357-372.

Hart SJ, Smith DJ, Clauge JJ. 2010. A multi-species dendroclimatic reconstruction of Chilko River streamflow, British Columbia, Canada. *Hydrological Processes* **24**: 2752-2761.

Haygreen JG, Bowyer JL. 1996. *Forest Products and Wood Science, 3rd Edition*, Iowa State University Press: Ames: IA.

Holmes RL, Adams RK, Fritts HC. 1986. *Tree-Ring Chronologies of Western North America: California, Eastern Oregon and Northern Great Basin, with Procedures used in the Chronology Development Work, Including User Manuals for Computer Programs COFECHA and ARSTAN. Chronology Series VI.* University of Arizona, Laboratory of Tree-Ring Research: Tucon, AZ.

Irvine JR, Fukuwaka M. 2011. Pacific salmon abundance trends and climate change. *ICES Journal of Marine Science*. DOI: 10.1093/icesjms/fsq199.

Jensen WB. 2007. The origin of the Soxhlet extractor. *Chemical Education Today* **84**: 1913-1914.

JISAO (Joint Institute for the Study of the Atmosphere and Ocean website). 2011. *Climate Data Archive*. http://jisao.washington.edu/data_sets/, [4 January, 2011].

Johnson KJ. 2010. *Late Holocene climate and glacier fluctuations in the Cambria Icefield area, British Columbia Coast Mountains*. Unpublished M.Sc. thesis, University of Victoria: Victoria, BC.

Kaufman CA. 2008. *Recent hydroclimate dynamics in southwest Alaska: understanding multidecadal climate variability through sedimentary process studies and varve sedimentology*. Unpublished M.Sc. thesis, Queen's University: Kingston, ON.

Kendrew WG, Kerr D. 1955. *The Climate of British Columbia and Yukon Territory*, Queen's Printer and Controller of Stationary: Ottawa, ON.

Kiffney PM, Bull JP, Feller MC. 2002. Climatic and hydrologic variability in a coastal watershed of southwestern British Columbia. *Journal of the American Water Resources Association* **38**: 1437-1451.

Koehler L, Smith DJ. 2011. Late Holocene glacial activity in Manatee Valley, southern Coast Mountains, British Columbia, Canada. *Canadian Journal of Earth Sciences* **48**: 1-17. DOI: 10.1139/E10-087.

Lamoureux SF, Stewart KA, Forbes AC, Fortin D. 2006. Multidecadal variations and decline in spring discharge in Canadian middle Arctic since 1550 AD. *Geophysical Research Letters* **33**: 1-4. DOI: 10.1029/2005GL024942.

Larocque SJ, Smith DJ. 2005a. A dendroclimatological reconstruction of climate since AD 1700 in the Mt. Waddington area, British Columbia Coast Mountains, Canada. *Dendrochronologia* **22**: 93-106.

Larocque, SJ, Smith DJ. 2005b. 'Little Ice Age' proxy mass balance records reconstructed from tree rings in the Mt Waddington area, British Columbia Coast Mountains, Canada. *The Holocene* **15**: 748-757.

Laroque CP. 2002. *Dendroclimatic response of high-elevation conifers, Vancouver Island, British Columbia*. Unpublished Ph.D. dissertation, University of Victoria: Victoria, BC.

Laroque CP, Smith DJ. 2003. Radial-growth forecasts for five high-elevation conifer species on Vancouver Island, British Columbia. *Forest Ecology and Management*, **183**: 313-325. DOI: 10.1016/SO378-1127(03)00110-5.

Luckman BH. 2003. Glacier fluctuation and tree-ring records for the last millennium in the Canadian Rockies. *Quaternary Science Reviews* **12**: 441-450.

MacHutchon AG, Himmer S, Davis H, Gallagher M. 1995. Temporal and spatial activity patterns among coastal bear populations. *Ursus* **10**: 539-546.

Mantua NJ, Hare SR, Zhang Y, Wallace JM, Francis RC. 1997. A Pacific interdecadal climate oscillation with impacts on salmon production. *Bulletin of the American Meteorological Society* **78**: 1069-1079.

Meidinger DV, Pojar J. 1991. In *Ecosystems of British Columbia, British Columbia Ministry of Forests Special Report Series No. 6*. Meidinger DV, Pojar J (eds). Victoria, British Columbia.

Moore RD. 1996. Snowpack and runoff responses to climatic variability, southern Coast Mountains, British Columbia. *Northwest Science* **70**: 321-333.

Moore RD, McKendry IG. 1996. Spring snowpack anomaly patterns and winter climatic variability, British Columbia, Canada. *Water Resources Research* **32**: 623-632.

Moore RD, Spittlehouse D, Whitfield P, Stahl K. 2010. Weather and climate. In *Compendium of Forest Hydrology and Geomorphology in British Columbia Volume 1 of 2*, Pike RG, Redding TE, Moore RD, Winkler RD, Bladon KD (eds). British Columbia Ministry of Forests and Range, Forest Science Program: Victoria; 47-84.

NCAR (National Center for Atmospheric Research website). 2011. *Niño Region 3 and Niño Region 3.4 SST Indices*. http://www.cgd.ucar.edu/cas/catalog/climind/Nino_3_3.4_indices.html, [4 January, 2011].

Nehlsen W, Williams JE, Lichatowich JA. 1991. Pacific salmon at the cross-roads: stocks at risk from California, Oregon, Idaho, and Washington. *Fisheries* **16**: 4-21.

Nijssen B, O'Donnell GM, Hamlet AF, Lettenmaier DP. 2001. Hydrologic sensitivity of global rivers to climate change. *Climatic Change* **50**: 143-175.

Overland JE, Adams JM, Bond NA. 1999. Decadal variability of the Aleutian Low and its relation to high-latitude circulation. *Journal of Climate* **12**: 1542-1548.

Perkins JA, Sims JD. 1983. Correlation of Alaskan varve thickness with climatic parameters, and use in paleoclimatic reconstruction. *Quaternary Research* **20**: 308-321.

Pearcy WG. 1992. *Ocean Ecology of North Pacific Salmonids*, University of Washington Press: Seattle, WA.

Peterson DL, Arbaugh MJ, Robinson LJ, Derderian BR. 1990. Growth trends of whitebark pine and lodgepole pine in a subalpine Sierra Nevada forest, California, USA. *Arctic and Alpine Research* **22**: 233-243.

Peterson DW, Peterson DL. 2001. Mountain hemlock growth responds to climatic variability at annual and decadal time scales. *Ecology* **82**: 3330-3345.

Peterson DW, Peterson DL, Ettl GJ. 2002. Growth responses of subalpine fir to climatic variability in the Pacific Northwest. *Canadian Journal of Forest Research* **32**: 1503-1517.

Philander, GS. 1990. *El Nino, La Nina and the Southern Oscillation*, Academic Press, London, UK.

Poff NL, Ward JV. 1989. Implications of streamflow variability and predictability for lotic community structure: a regional analysis of streamflow patterns. *Canadian Journal of Fisheries and Aquatic Sciences* **46**: 1805-1818.

Rand PS, Hinch SG, Morrison J, Foreman MGG, MacNutt MJ, MacDonald JS, Healey MC, Farrell AP, Higgs DA. 2006. Effects of river discharge, temperature and future climates on energetics and mortality of adult migrating Fraser River sockeye salmon. *Transactions of the American Fisheries Society* **135**: 655-667.

Raper SCB, Briffa KR, Wigley TML. 1996. Glacier change in northern Sweden from AD 500: a simple geometric model of Storglaciaren. *Journal of Glaciology* **42**: 341-351.

Schindler DW. 1997. Widespread effects of climatic warming on freshwater systems in North America. *Hydrological Processes* **11**: 1043-1067.

Schindler DW. 2001. The cumulative effects of climate warming and other human stresses on Canadian freshwaters in the new millennium. *Canadian Journal of Fisheries and Aquatic Sciences* **58**: 18-29.

Schweingruber FH, Fritts HC, Braker OU, Drew LG, Schar E. 1978. The x-ray technique as applied to dendrochronology. *Tree-Ring Bulletin* **38**: 61-91.

Shabbar A, Khandeker M. 1996. The impact of El Niño-Southern Oscillation on the temperature field over Canada. *Atmosphere-Ocean* **34**: 401-416.

Shabbar A, Bonsal BR, Khandeker M. 1997. Canadian precipitation patterns associated with the Southern Oscillation. *Journal of Climate* **10**: 3016-3027.

Slaney TL, Hyatt KD, Northcote TG, Fielden RJ. 1996. Status of anadromous salmon and trout in British Columbia and Yukon. *Fisheries* **21**: 20-35.

Smith DJ, Laroque CP. 1998. Mountain hemlock growth dynamics on Vancouver Island. *Northwest Science* **72**: 67-70.

Smith S. 2001. Water Resources. In *British Columbia, the Pacific Province: Geographical Essays*, Wood C (ed). Western Geographical Press: Victoria; 65-82.

Spilsted B, Spencer B. 2009. Documentation of North Coast (Statisical Areas 1 to 6) salmon escapement information. *Canadian Manuscript Report of Fisheries and Aquatic Sciences 2808*: 1-66.

Splechtna BE, Dobry J, Klinka K. 2000. Tree-ring characteristics of subalpine fir (*Abies lasiocarpa* (Hook.) Nutt.) in relation to elevation and climate fluctuations. *Annals of Forest Science* **57**: 89-100.

Stahl K, Moore RD. 2006. Influence of watershed glacier coverage on summer streamflow in British Columbia, Canada. *Water Resources Research* **42**: 1-5. DOI: 10.1029/2006WR005002.

Stahl K, Moore RD, McKendry IG. 2006. The role of synoptic-scale circulation in the linkage between large-scale ocean-atmospheric indices and winter surface climate in British Columbia, Canada. *International Journal of Climatology* **26**: 541-560.

Stewart IT. 2009. Changes in snowpack and snowmelt runoff for key mountain regions. *Hydrological Processes* **23**: 78-94.

Stockton CW, Fritts HC. 1973. Long-term reconstructions of water level changes for Lake Athabasca by analysis of tree rings. *Water Resources Bulletin* **9**: 1006-1027.

Stokes MA, Smiley TL. 1964. *An Introduction to Tree-ring Dating*, University of Chicago Press: Chicago, IL.

Sugimoto T, Tadokoro K. 1997. Interannual-interdecadal variations in zooplankton biomass, chlorophyll concentration and physical environment in the subarctic Pacific and Bering Sea. *Fisheries Oceanography* **6**: 74-93.

Torrence C, Compo GC. 1998. A practical guide to wavelet analysis. *Bulletin of the American Meteorological Society* **79**: 61-78.

Trenburth KE, Hurrell JW. 1994. Decadal atmosphere-ocean variations in the Pacific. *Climate Dynamics* **9**: 303-319.

WSC (Water Survey of Canada website) 2011. *HYDAT Archived Hydrometric Data*. Environment Canada, Water Survey of Canada: Ottawa, ON; http://www.wsc.ec.gc.ca/applications/H2O/index-eng.cfm, [20 December, 2010].

Watson E, Luckman BH. 2004. Tree-ring-based mass-balance estimates for the past 300 years at Peyto Glacier, Alberta, Canada. *Quaternary Research* **62**: 9-18.

Watson E, Luckman BH. 2005. An exploration of the controls of pre-instrumental streamflow using multiple tree-ring proxies. *Dendrochronologia* **22**: 225-234.

Whitfield PH. 2001. Linked hydrologic and climate variations in British Columbia and Yukon. *Environmental Monitoring and Assessment* **67**: 217-238.

Whitfield PH, Moore RD, Fleming SW, Zawadzki A. 2010. Pacific Decadal Oscillation and the hydroclimatology of western Canada – review and prospects. *Canadian Water Resources Journal* **35**: 1-28.

Wigley TML, Briffa KR, Jones PD. 1984. One the average value of correlated time series, with applications in dendroclimatology and hydrometeorology. *Journal of Climate and Applied Meteorology* **23**: 201-213.

Wood CJB, Corpé C. 2001. Fisheries. In *British Columbia, the Pacific Province: Geographical Essays*, Wood CJB (ed). Western Geographical Press: Victoria; 329-344.

Woodhouse CA. 2003. A 431-yr reconstruction of western Colorado snowpack from tree rings. *Journal of Climate* **16**: 1551-1561.

Woodhouse CA, Gray ST, Meko DM. 2006. Updated streamflow reconstructions for the Upper Colorado River Basin. *Water Resources Research* **42**: WO5415, DOI: 10.1029/2005WR004455.

Woodward A, Silsbee DG, Schreiner EG, Means JE. 1994. Influence of climate on radial growth and cone production in subalpine fir (*Abies lasiocarpa*) and mountain hemlock (*Tsuga mertensiana*). *Canadian Journal of Forest Research* **24**: 1133-1143.

Appendices

Appendix A.
Climate Reconstruction Calibration Diagrams

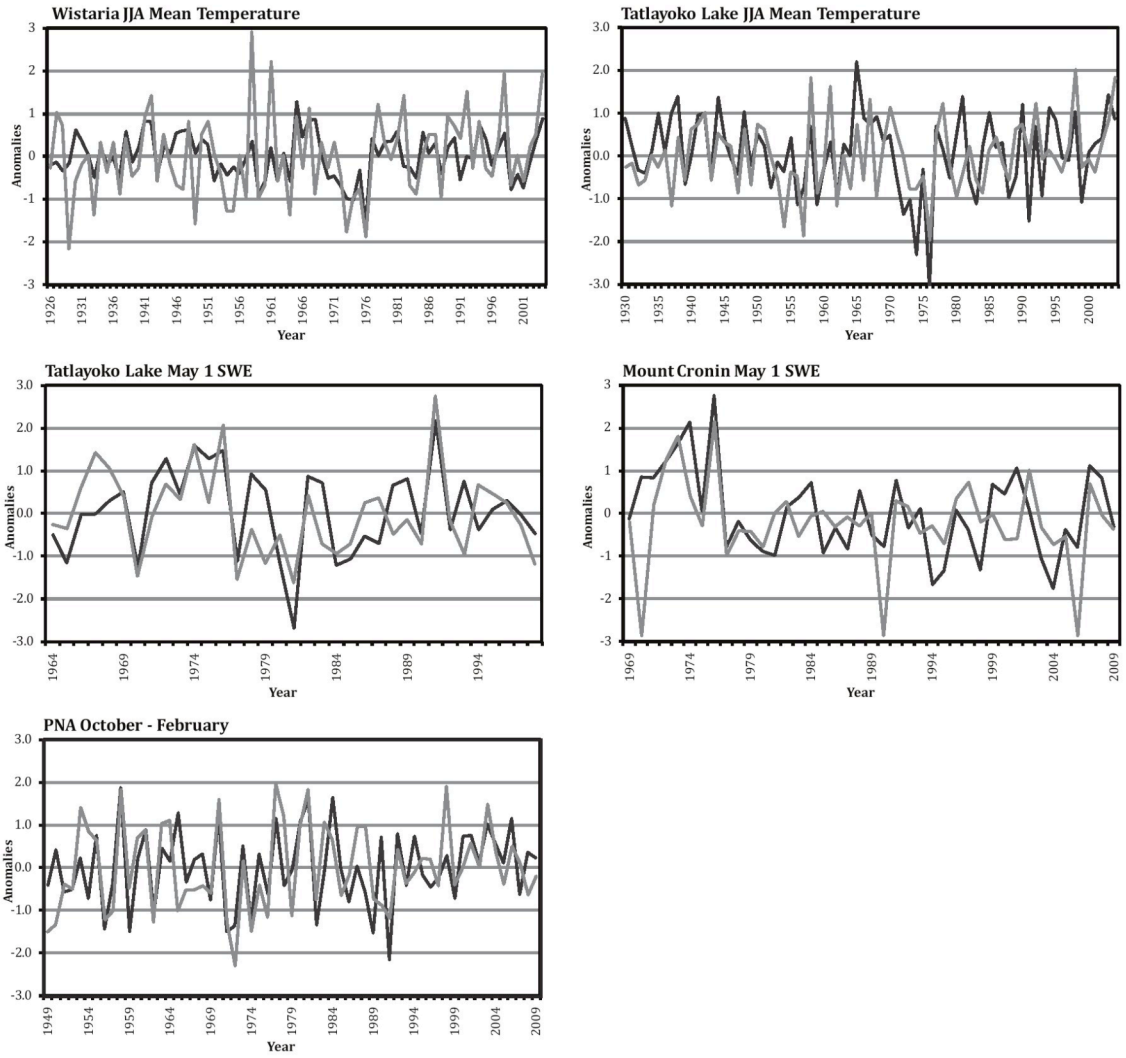

Figure A.1 Comparison between reconstructed (black line) and instrumental (gray line) records of summer temperature, SWE and PNA during the calibration period

Appendix B.
Climate Reconstruction Wavelet Power Spectrum Diagrams

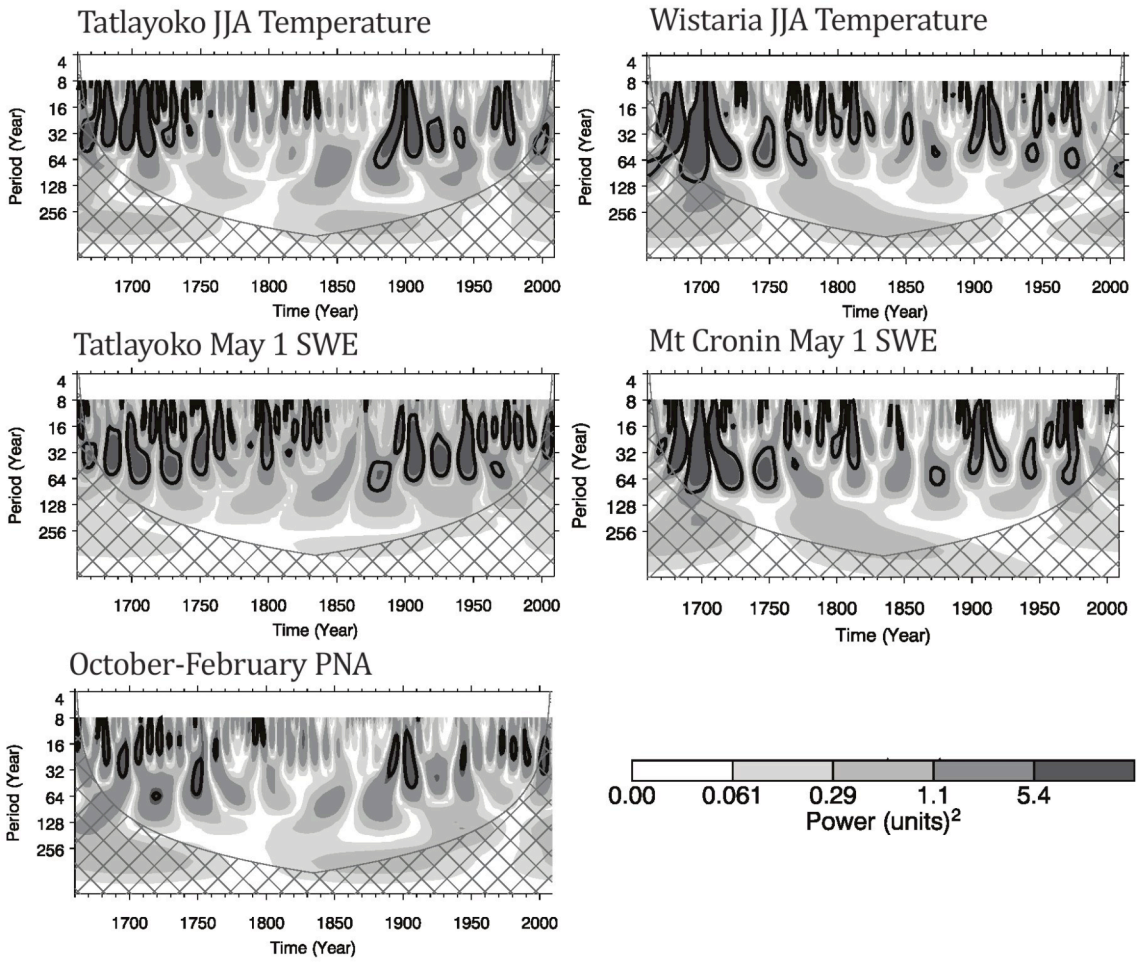

Figure B.1 Wavelet power spectrum for temperature, SWE and PNA reconstructions. The wavelet power spectrum uses a Gaussian-2 function. Cross-hatched regions of the wavelet diagrams represent the cone of influence where zero-padding of the data was used to reduce variance. Black contours indicate significant modes of variance with a 5% significance level using an autoregressive lag-1 red-noise background spectrum (Torrence and Compo, 1998).

Reference

Torrence C, Compo GC. 1998. A practical guide to wavelet analysis. *Bulletin of the American Meteorological Society* **79**: 61-78.

Appendix C.
Exploratory Model of Salmon Abundance Using Catch Records

An exploratory model explaining the long-term dynamics of Pacific salmon abundance was constructed using tree-ring records and a short (23 years) record of total salmon return (escapement estimates and commercial fisheries catch estimates). Data was retrieved from a report written by the Skeena Independent Science Review Panel (Walters *et al.*, 2008). Initial correlation analysis indicated that the residual yellow cedar (YC) chronology ($r = -0.586$, $p = 0.003$) and the standardized regional Douglas-fir (DF) chronology ($r = -0.521$, $p = 0.011$) were appropriate predictor variables for modelling a composite record of chinook, sockeye and pink salmon returning to the Skeena River basin. Methods used for the correlation analysis and reconstruction were the same as those outlined in both Chapters 2 and 3. The resultant model produced comparatively stronger model statistics ($r = 0.698$; $r^2 = 0.483$) than the models presented in Chapter 3. A visual assessment of modelled and actual trends during the calibration period illustrates that the model is proficient at capturing trends in total salmon run records (Figure C.1). As model statistics for this composite record were deemed to have significant predictive capabilities the model was reconstructed back to 1660 AD, after which the DF chronology sample depth decreases and affects the expressed population signal (Figure C.2).

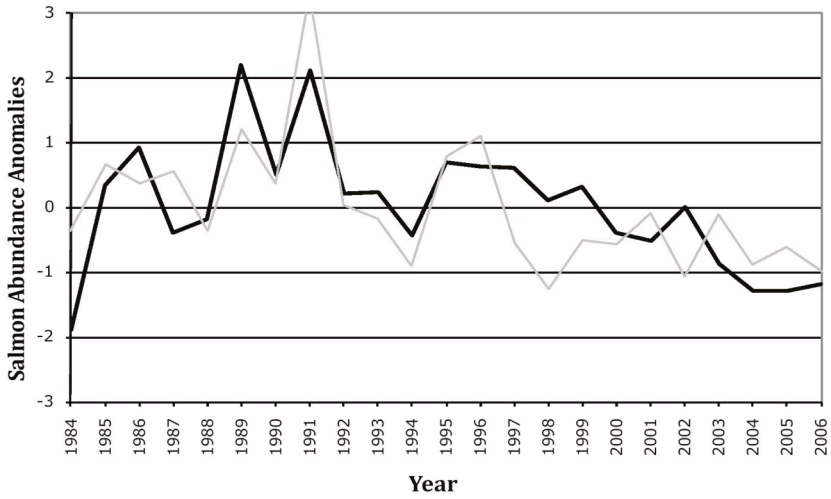

Figure C.1 Comparison between reconstructed (black) and instrumental (gray) records of Pacific salmon abundance for Chinook, pink and sockeye salmon returning to the Skeena River (including both escapement and catch records) during the calibration period.

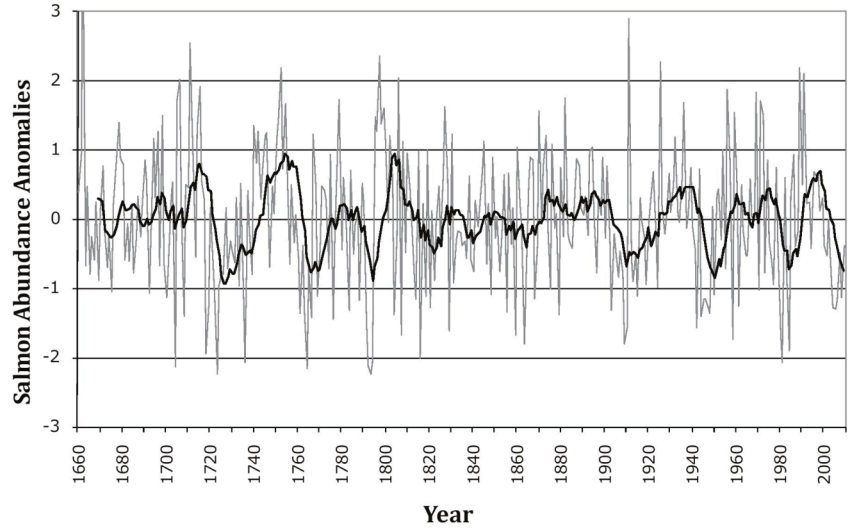

Figure C.2 Reconstruction of Pacific salmon abundance (Chinook, pink and sockeye) for the Skeena River back to 1660 AD, calibrated from salmon catch and escapement records.

Reference

Walters CJ, Lichatowich JA, Peterman RM, Reynolds JD. 2008. Report on the Skeena Independent Science Review Panel. A report to the *Canadian Department of Fisheries and Oceans and the British Columbia Ministry of Environment*, 144 p.

Appendix D.
Exploratory Correlation Analyses with Ring-Density Chronologies

Exploratory correlation analyses were completed between hydroclimate variables and standardized yellow cedar (YC) and Douglas-fir (DF) ring-width and ring-density chronologies. The purpose of these analyses was to demonstrate the relative strength of density chronologies compared with ring-width chronologies. Correlations were considered statistically significant at the 0.05 level. Compared results between the density and ring-width chronologies indicated that wood density often captured signals not recorded by ring-width and/or captured hydroclimate signals with more strength than their ring-width counterparts. An example of this is provided in Table D.1 below. Recognizing the strength of the wood density signal, it is recommended that future tree-ring modelling studies consider collecting wood density chronologies.

Table D.1 Comparative strength of individual-site ring-density and ring-width chronologies when correlated to temperatures at Tatlayoko Lake

Data			Mean			
			June	July	August	JJA
YC	max density	r	0.243	0.165	0.422	0.400
		p	0.036	0.157	0.000	0.000
	width	r	-0.018	0.081	-0.026	0.014
		p	0.875	0.488	0.827	0.907
Data			October-April Temperature			
			Min	Max	Mean	
DF	min density	r	-0.444	-0.445	-0.459	
		p	0.000	0.000	0.000	
	width	r	0.359	0.394	0.380	
		p	0.002	0.000	0.001	

r – correlation, p – significance

Appendix E.
Century-Scale Growth of Yellow Cedar and Whitebark Pine Trees

The yellow cedar (YC) and regional whitebark pine (WBP) chronologies presented in this thesis contain a distinctive century-scale trend in ring-width growth (Figure E.1). Throughout the past six centuries there have been six periods where WBP ring-widths reached a growth minimum. Minima marked the early- and late-1400s, the late-1500s, the early-1700s, the mid-1800s and the late-1900s. Following these episodes of minimum growth WBP ring-widths steadily increased until they reached a maximum after which they rapidly entered another minimum growth phase.

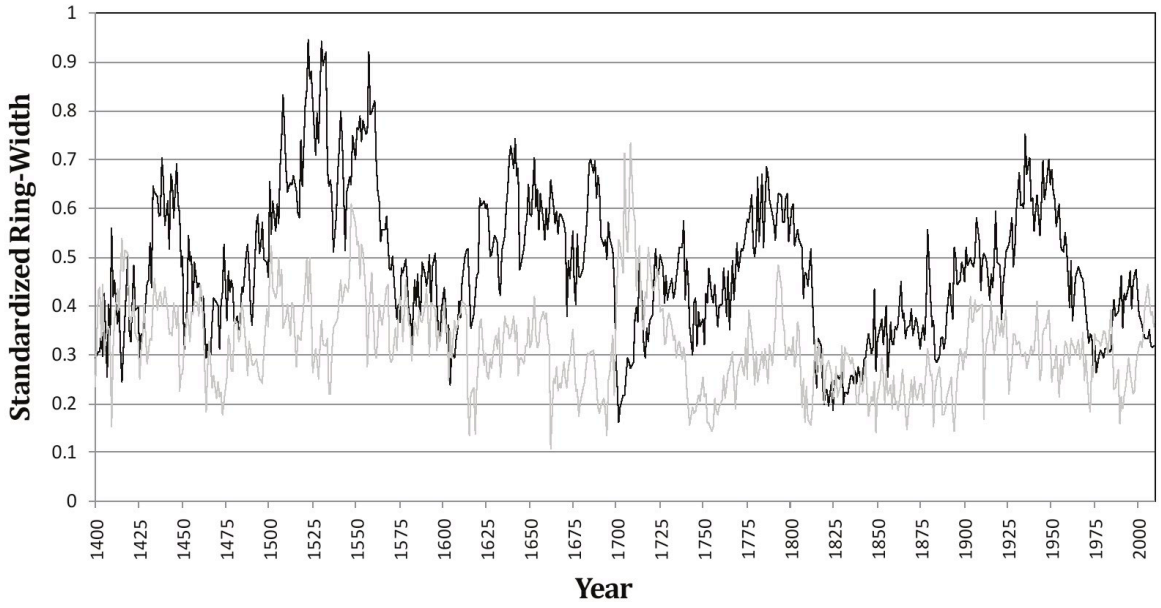

Figure E.1 Growth anomalies of the yellow cedar (gray line) and whitebark pine (black line) ring-width chronologies.

The YC ring-widths displayed similar low-frequency trends although the pattern was less apparent. Over the six centuries examined YC ring growth has shifted from 'in synchrony' to 'out of synchrony' with WBP ring growth. The strong out-of-phase response marking the early-1700s provides a clear example of this behavior. Considering the physical distance between sampled stands, the synchronous shifts and reverse shifts present in the ring-width data were interpreted to be regional responses to a large-scale forcing rather than stand-level responses to site-specific changes.

Closer visual inspection of the ring-width data revealed a second shorter-frequency cycle that appears to be superimposed on the century-scale growth trend. Again, this cycle was more apparent in the WBP chronology and became particularly evident during the periods of steadily increasing ring-widths between minimums. Visual analysis of the steadily increasing ring-widths between the last two minima in WBP growth (during the 1820s and 1970s) revealed several smaller declines in growth during the 1880s and mid-1920s. The timing of these events roughly matches recognized shifts in large-scale ocean and atmospheric forcings described by the Pacific Decadal Oscillation and the Pacific North America pressure pattern (D'Arrigo *et al.*, 2001; Mantua *et al.*, 1997). Regime-shifts in sea surface temperatures and North Pacific pressure anomalies mark the mid-1920s, the late-1940s and the late-1970s (Stahl *et al.*, 2006). Notable declines in WBP growth occurred during shifts in PDO from a negative phase to a positive phase (shifts in the mid-1920s and late-1970s) (Mantua *et al.*, 1997). The shift from positive PDO to negative PDO phase in the late-1940s (Mantua *et al.*, 1997) was also identifiable as a peak in WBP growth. During this period the

trends were less apparent in the YC chronology and are therefore not discussed. Although a similarity was visually identified between WBP ring growth and the timing of regime-shifts in large-scale climate forcings, further detrending of the ring-width data is required to first remove the century-scale trend before this relationship can be further assessed.

A wavelet analysis was completed on the YC and WBP tree-ring chronologies to evaluate the frequency of the century-scale trend (Figure E.2). Results exposed a low-frequency (approximately 60-120 years) cycle in WBP and YC ring-width data. A second lower-frequency cycle also characterized tree-ring records and had a frequency period exceeding 200 years.

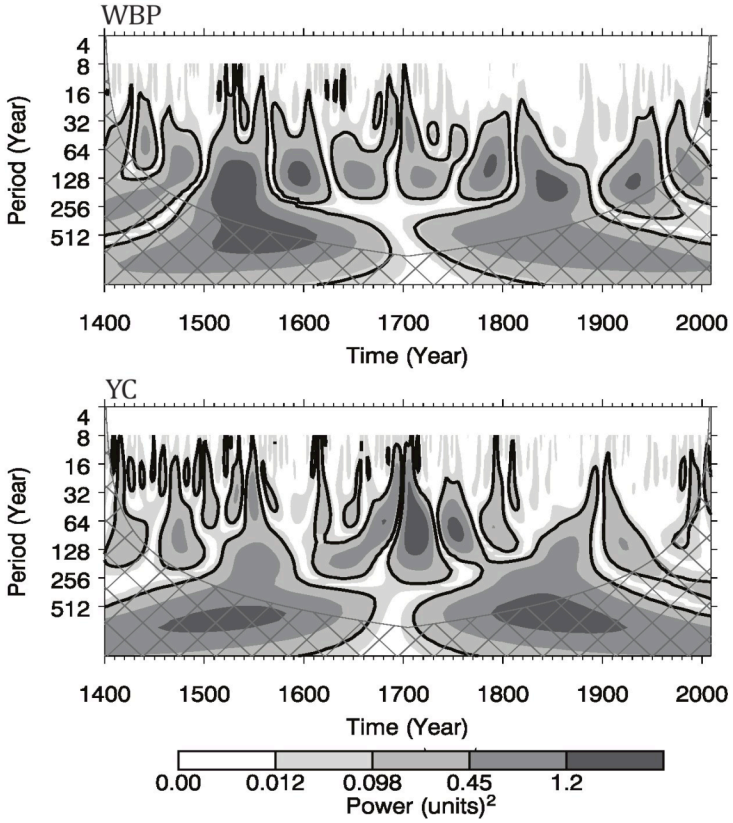

Figure E.2 Wavelet power spectrum for yellow cedar and whitebark pine chronologies. The wavelet power spectrum uses a Gaussian-2 function. Cross-hatched regions of the wavelet diagrams represent the cone of influence where zero-padding of the data was used to reduce variance. Black contours indicate significant modes of variance with a 5% significance levels using an autoregressive lag-1 red-noise background spectrum (Torrence and Compo, 1998).

The origin of the forcing mechanism producing the century-scale growth trends in both the YC and WBP chronologies is unknown. Recent dendroclimatic research in central Asia describes a similar low-frequency pattern of growth for Juniper trees (Raspopov *et al.*, 2008). Raspopov *et al.* (2008) argued that this low-frequency growth pattern was a response to changes in annual sunspot numbers associated with the de Vries (~200 year) solar cycle. To test this hypothesis, Raspopov *et al.* (2008) transformed tree-ring and sunspot data using a 180-230 year wavelet filter. In an earlier study, Ogurtsov *et al.* (2002) similarly looked for higher-frequency solar variations describing the Schwabe solar cycle in tree-ring data with using a 64-128 year wavelet filter.

To assess whether solar cycles may also explain the low-frequency patterns in YC and WBP growth, wavelet transformations of the chronologies were completed using a 70-120 year frequency filter and a 150-250 year frequency filter (Figure E.3). Sunspot numbers were obtained from the National Oceanic and Atmospheric Administration (NOAA, 2011) and were similarly filtered for low-frequency patterns.

Visual inspection of the wavelet-filtered ring-width and sunspot records did not yield conclusive connections between solar activity and anomalies in tree-ring growth. Although periods of depressed ring-width in the YC and WBP chronologies occurred during episodes of well-recognized minimums in sunspot activity including during the Spörer Minimum (1450-1550 AD), the Maunder Minimum (1645-1715 AD) and the Dalton Minimum (1790-1820 AD); there were also intervals of enhanced ring growth during the Spörer and Maunder minimas.

Moreover, similar magnitude intervals of depressed ring growth occurred during periods of time defined by higher sunspot activity.

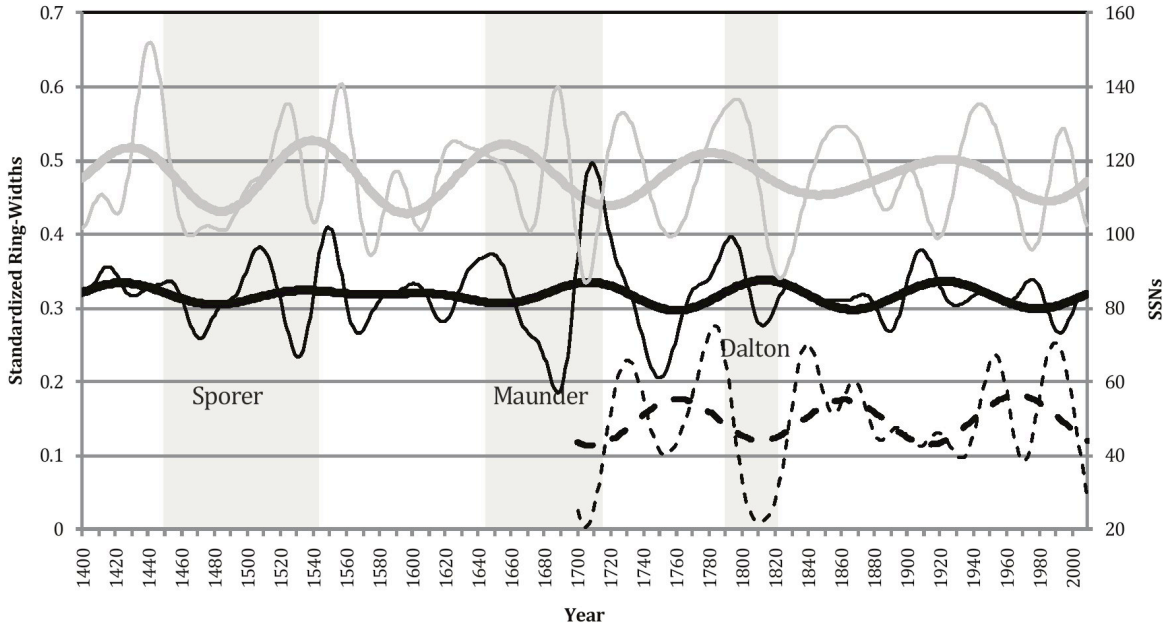

Fig. E.3 Wavelet-filtered records of whitebark pine (solid gray lines) yellow cedar (solid black lines) and sunspot numbers (dashed black lines). Data have been transformed twice, the first transformation, represented with the thin lines, involved running a 70-120 year frequency wavelet-filter. The second transformation, represented with the thicker lines, involved running a 150-250 year frequency wavelet-filter. Shaded areas represent recognized intervals of sunspot minima.

Exploratory investigations on YC and WBP ring-width data were largely inconclusive. The 60-120 year frequency cycle identified in the ring-width data is likely related to regime shifts in atmospheric and oceanic circulation patterns. This assessment requires further data transformation before a robust conclusion can be obtained. The possibility of a relationship between ring-width and variations in solar activity also requires further analysis.

References

D'Arrigo RD, Jacoby GC, Free RM. 1992. Tree-ring width and maximum latewood density at the North American treeline: parameters of climate change. *Canadian Journal of Forest Research* **22**: 1290-1296.

Mantua NJ, Hare SR, Zhang Y, Wallace JM, Francis RC. 1997. A Pacific interdecadal climate oscillation with impacts on salmon production. *Bulletin of the American Meteorological Society* **78**: 1069-1079.

NOAA (National Oceanic and Atmospheric Administration). 2011. *Sunspot Numbers*. www.ngdc.noaa.gov/nndc/struts/results?t=102827&s=5&d=8,430,9, [4 April, 2011].

Ogurtsovi MG, Kocharovi GE, Lindholm M, Meriläinen J, Eronen M, Nagovitsyn YA. Evidence of solar variation in tree-ring-based climate reconstructions. *Solar Physics* **205**: 403-417.

Raspopov OM, Dergachev VA, Esper J, Kozyreva OV, Frank D, Ogurtsov M, Kolström T, Shao X. 2008. The influence of the de Vries (~200-year) solar cycle on climate variations: Results from the Central Asian Mountains and their global link. *Palaeogeography, Palaeoclimatology and Palaeoecology* **259**: 6-16.

Stahl K, Moore RD, McKendry IG. 2006. The role of synoptic-scale circulation in the linkage between large-scale ocean-atmospheric indices and winter surface climate in British Columbia, Canada. *International Journal of Climatology* **26**: 541-560.

Torrence C, Compo GC. 1998. A practical guide to wavelet analysis. *Bulletin of the American Meteorological Society* **79**: 61-78.